Fatigue Life Analysis of Holed Component in Aircraft Stuctures

By

Muhammad Zulfaqqar bin Mohd Kasim

14367

Dissertation submitted in fulfilment of

the requirement for the

Bachelor of Engineering (Hons.)

(Mechanical)

May 2015

Universiti Teknologi PETRONAS

Bandar Seri Iskandar

32610 Tronoh,

Perak Darul Ridzuan

TABLE OF CONTENT

ABSTRACT

Aircraft structure with holes was thought to have a significant impact towards fatigue life. Holes had been stress concentrators where high magnitude of stress will be focused around it and potentially be the fatigue crack imitation site. Stress and fatigue analysis were done through finite element simulation to see the effect of stress concentration upon the fatigue life of a plate-with-hole model. This model has been a simple representation of the complex holed aircraft structures. It was found out that the result obtained was consistent to the assumptions made where parts with stress concentration will have a shorter fatigue life due to the severity of damage it face as cyclic loading is being applied to it. The current practice of fatigue life prediction is usually through the process of full scale fatigue simulation which is a cost intensive and a very time consuming process and through lab experiment which considerably complicated and time consuming as well. This study had been focusing on creating a fatigue life estimation that is simple and reliable. In this study, a method that highly focuses on the usage of finite element software has been used and it was found out that the result is convincingly simple and reliable with only 0.5% error.

1. INTRODUCTION

1.1 Background of study

Metal fatigue is the most common type failure mechanism which occurs in aircraft structures. According to data gathered by the *materialstoday* journal, published in November 2002, metal fatigue had occupied 55% of the percentage of failure modes in an aircraft, signifying that, metal fatigue is a serious issue within aviation industry. There are several factors which could lead to metal fatigue in design, such as the size factor, the surface roughness, metallurgical defects within grains, and stress concentrations. However, for this study, focus will be thoroughly given to the stress concentration factors and to be more specific, stress concentrators in the form of holes.

Through non-destructive tests which were done in the entire aircraft section, fatigue sign in the form of small cracks were mostly found in the area of holed parts. These holed parts could be the rivet holes, bolt holes, panel opening cut outs, window frames, and door frames. Wherever there are openings or discontinuity on the fuselage, wings, frames or other major aircraft structures, there will always be stress concentrations. A simulation was done to see how the stress concentrator in the form of hole affects the fatigue life of the structure and the it was further discussed in result in discussion section.

In addition to that, a huge emphasize was also given to the development of the simpler and reliable fatigue life prediction of aircraft structures. Current method of fatigue life prediction which was used by the aviation industry is currently very costly and time consuming (further discussed in problem statement part) and this study was done to develop a simpler method of estimation which will hopefully be useful in industry in cutting costs and time consumptions as well as to provide a simpler method of analysis for future researches.

As established in S.J. Findlay and N.D. Harrison in their article, *Why aircraft fail* published in November 2002 edition of *materialstoday* journal, the fatigue failure process involves three phases. First, the crack initiation phase which occur first and followed by the crack propagation phase, at which the crack spreads. When the crack reaches the critical size, the final unstable rapid crack propagation occurs, which will leads to the third and final phase which is the failure phase. This study was only focusing onto the crack initiation phase, which is the phase where the microcracks just start to appear after several cycles of loading input. This particular phase is very important for analysis because it reflects of the real durability of the structure itself. Second and third phases of the fatigue life are no longer relevant for this analysis because the rate of damage will only accelerate up until the structure failure since the crack was already formed (in the first phase: crack initiation). For the fatigue life prediction of the holed aircraft structure, strain-life method via Finite Element analysis and analytical analysis approach will be utilised as the main analysis tool. Details for the planned analysis and simulation methods were further discussed in the following methodology section.

1.2 Problem statement

The estimation of fatigue life of an aircraft could be done through full scale fatigue testing by introducing loading histories that are approximately similar like the real operation condition. This method had proven to be reliable in providing quite a good fatigue life estimates and was widely used by aircraft manufacturers. However, despite its reliability, this method is very time consuming. A full-scale fatigue test could take months to complete and to get results. Additionally, the full-scale fatigue test could be very costly as it requires the whole aircraft to be tested. Having this fact, the full scale fatigue test was absolutely not viable for research purposes and this demands an alternative which is fairly simple and reliable enough to be used as a research tool for the metal fatigue, especially in aircraft structures.

As mentioned earlier in the background of study section, it is very common to find the fatigue signs at the holed part of the aircraft structures. This holed part includes, the rivet holes, bolt holes, lugs, fuselage cut outs (window and door frames) and etc. These holes were known to be stress concentrators in aircraft structures, in which the stress in this area is multiple times higher than area without any cut outs or open holes. Upon cycles of stresses, these holed areas are the most susceptible place to experience metal fatigue, especially at the structural parts which have to bear high magnitude of loading frequently. So, it is crucial to investigate further about how the presence of stress concentrators affects the fatigue life of aircraft structures.

1.3 Objective of study

Through the issues stated earlier in the problem statement section, several objectives were devised for this study which will cover all the stated issues. The objectives are;

- To provide a fairly simple and reliable method to estimate the aircraft structure's fatigue life.

- To determine how does the presence of stress concentrators (holes) could affect the fatigue life of aircraft structures.

1.4 Scope of study

As stated in the objective part, this study is mainly to develop a simple and reliable fatigue life prediction of aircraft structures from the existing knowledge of fatigue predictions developed by the early researches and also to determine how does the presence of hole in aircraft structures affects the fatigue life of it. There are several studies done previously regarding this topic and this study had been using them as references and guide in ensuring the result produced through the analysis is proper and accurate.

1.4.1 Determination of type of structure and materials to be analysed

Focus and attention will be given to the <u>holed aircraft structures/component parts</u> which some of them are very critical in aircraft operation. The reason for this particular type of structure was chosen is due to the presence of hole which may act as stress concentrator in the structure and is highly susceptible to fatigue damage. To study this, a simple virtual model of plate with a hole will be made to represent the holed aircraft structure or component parts such as the structural frame (stringers), aircraft skin, bulkheads, lugs and attachment points and it will be tested through finite element (FE) method to see the stress reaction upon this type of structure and the effect of this stress concentrator to the overall life of the structure under the simulated working condition.

SAE 1045 (medium carbon steel) had been chosen as the material of choice to be tested in this analysis. The main reason for this material had been chosen is mainly to get a material match for result validation process and this validation process will be done by comparing the result gained from this study to previous research work's results. In this study, the SAE 1045 steel is being virtually tested under the tensile stress through finite element (FE) analysis which mimics the stress condition of the pressurized fuselage in an aircraft. In addition to that, the similar method which was utilised for the simple plate-with-hole model was also used to one of the real-life component in aircraft structure, made up of 7075-T6 Aluminium alloy (commonly used material in aircraft) that has holes associated to the structure to estimate its fatigue life as a real-life case example.

Depicted in the following pages are the examples of holed structures/parts that are exists in aircrafts;

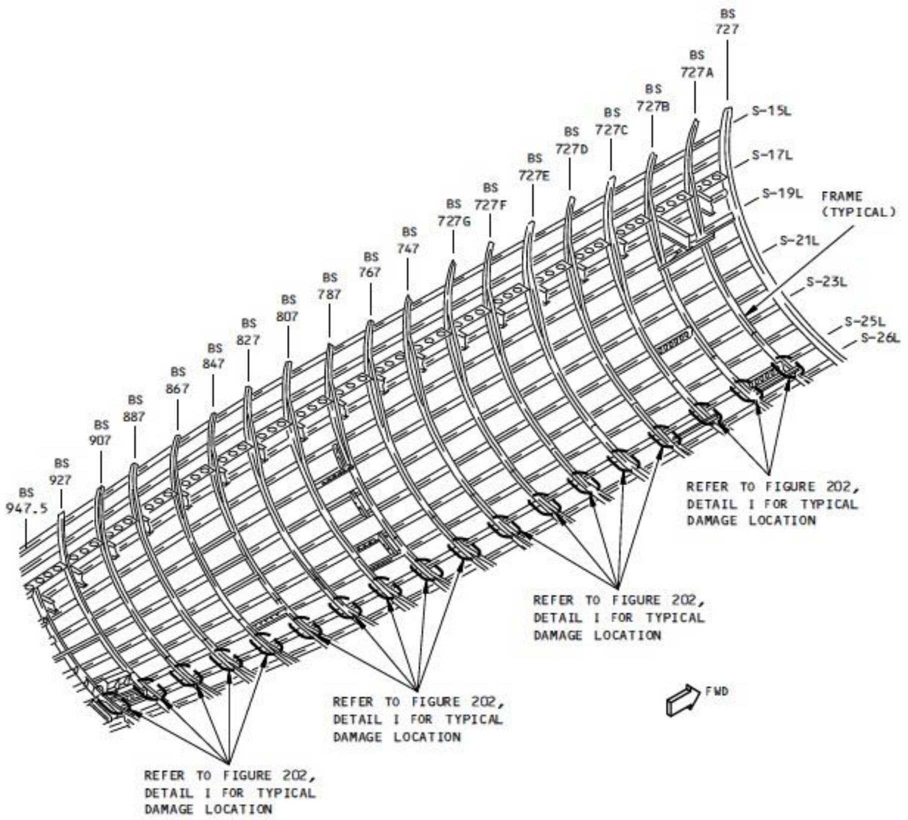

Figure 1: Frame of Boeing 737-400 aircraft retrieved from Boeing 737-400 Structure Repair Manual (SRM), Chapter 53: Fuselage, Subject 53-00-07 p.202

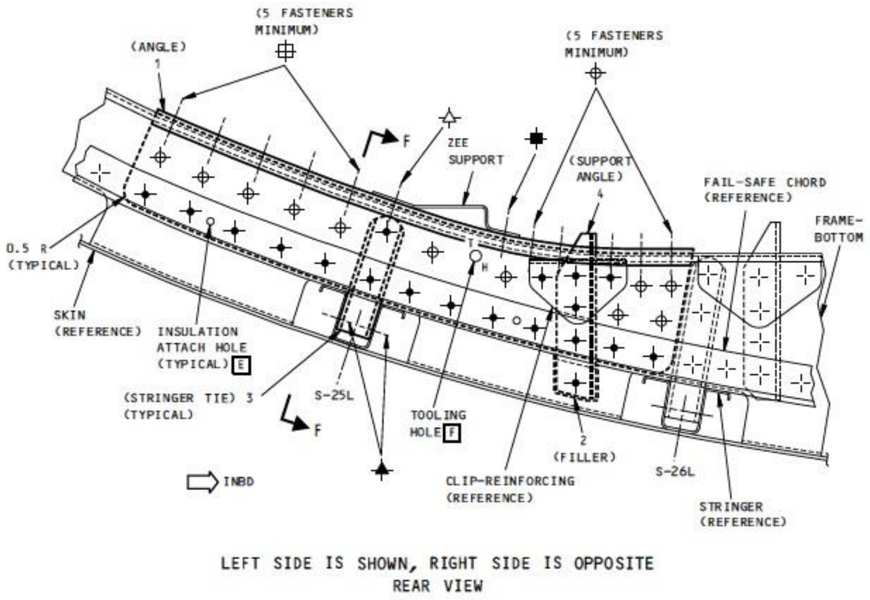

Figure 2: Side view of the frame of Boeing 737-400 aircraft retrieved (frame with fastener holes) from Boeing 737-400 Structure Repair Manual (SRM), Chapter 53: Fuselage, Subject 53-00-07 p.203

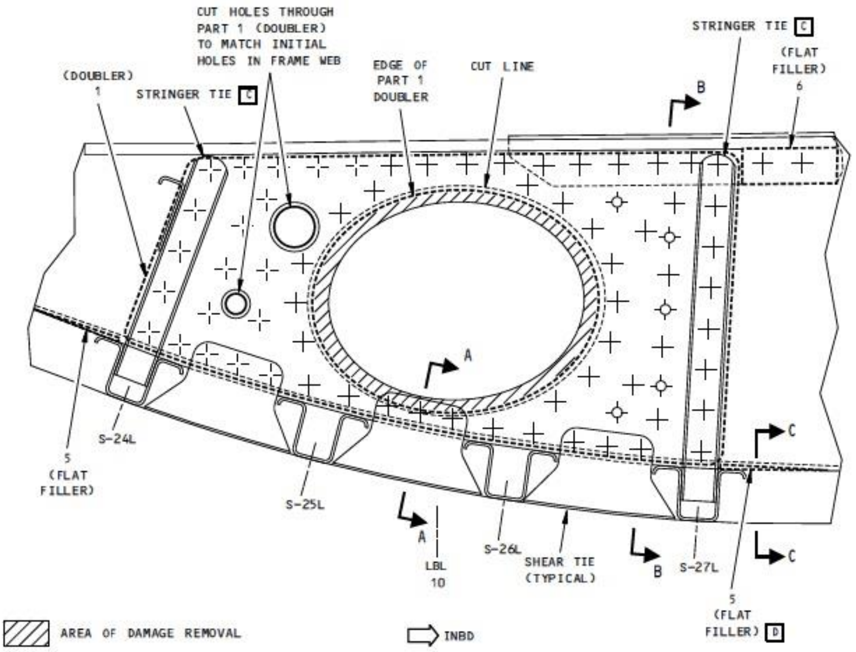

Figure 3: Holed frame part of Boeing 737-400 aircraft retrieved from Boeing 737-400 Structure Repair Manual (SRM), Chapter 53: Fuselage, Subject 53-80-07 (fuselage frames) p.204

1.4.2 Finite Element (FE) analysis and analytical method in stress analysis and fatigue life estimation

Both analytical calculations and Finite Element (FE) analysis were associated along with this method. In this research work, a method of fatigue life analysis that emphasizes on heavy usage of Finite Element (FE) and analytical analysis instead of full-scale/small-scale test was done in order to solve the high cost and time consumption to get the estimation of fatigue life result. Finite Element (FE) method which was adopted through the usage of ANSYS workbench 15.0.7 software is important for the stress analysis of the model where the effect of localized stress (stress concentration) in holed location of model was observed. Additionally, FE was also used to find the maximum local stress that is vital for the fatigue life calculation. Meanwhile, simple analytical calculations were utilized to calculate the fatigue cycles, fatigue cumulative damage, and several other parameters by applying the related governing equations, rules, and theories.

1.4.3 Seeking improvement for current fatigue life estimation method

During the course of this study too, a lot of research were done through several other related research works, text books, journals and articles that are related to this topic to help further increase the understanding of the topic and might as well find a way to further improve the established method produced by the earlier study such as Maksimovic's and etc. in order to achieve a more relevant and accurate results. Any input which might be useful in providing more accurate results and might be useful in the simplification process of the fatigue life estimation method obtained through these sources will be taken into consideration in the research and will be adjusted accordingly to suit the designed method.

2. LITERATURE REVIEW

2.1 Fatigue life prediction through local stress-strain concept

The local stress-strain concept was used as a tool to establish a simpler and a more reliable way to create a fatigue life prediction for aircraft structures. The basis for the local stress-strain approach is the local fatigue response of the material at the critical point (site of crack initiation) is comparable to the fatigue response of a small, simpler-shaped smooth specimen subjected to the same cyclic of strains and stresses. What the premise above meant, it is possible to determine the cyclic stress-strain response of the critical material through the simpler-shaped smooth specimen, by replicating the same load history applied on the critical material. It is to be noted that the phenomena of cyclic hardening, cyclic softening, and the sequential loading accumulates the fatigue damage was presumed to be at the same point the critical point (crack initiation site) in the structural component which to be simulated. The elastic-plastic behaviour will need to be addressed properly as well during while utilising this concept. (Maksimovic, 2005).

2.2 Von Mises Criterion

Von Mises criterion will be the basis in order to obtain the equivalent strain. The equation below is the basic equation from the Von Mises hypothesis which was also known as the Octahedral Shear strain theory (Fatemi, 2010) and it will be derived according to the ASME Boiler and Pressure Vessel code Procedure (1988) to find the equivalent stress range. This basis equation was composed using the Von Mises criterion, axial strains and shear strains;

$$\varepsilon_{eq,a} = \frac{1}{(1+\nu)\sqrt{2}}\left(\left(\varepsilon_{1,a} - \varepsilon_{2,a}\right)^2 + \left(\varepsilon_{2,a} - \varepsilon_{3,a}\right)^2 + \left(\varepsilon_{3,a} - \varepsilon_{1,a}\right)^2\right)^{1/2} \quad (1)$$

In the formula above (1) $\varepsilon_{1,a}$, $\varepsilon_{2,a}$, $\varepsilon_{3,a}$ are mean of the three main strains and ν is the Poisson's ratio. Meanwhile, the derived equation is as follows;

$$\Delta\varepsilon_{eq} = \frac{1}{(1+\nu)\sqrt{2}}\left(\left(\Delta\varepsilon_x - \Delta\varepsilon_y\right)^2 + \left(\Delta\varepsilon_y - \Delta\varepsilon_z\right)^2 + \left(\Delta\varepsilon_z - \Delta\varepsilon_x\right)^2 + 6\left(\Delta\varepsilon_{xy}^2 + \Delta\varepsilon_{yz}^2 + \Delta\varepsilon_{xz}^2\right)\right) \quad (2)$$

Next, by utilising the static yield theory of multi-axial loading and Von Mises criterion, the equation derived to get the equivalent multi-axial stress range is:

$$\Delta S_{eq} = \frac{1}{2}\left(\left(\Delta S_1 - \Delta S_2 \right)^2 + \left(\Delta S_2 - \Delta S_3 \right)^2 + \left(\Delta S_1 - \Delta S_3 \right)^2 \right)^{1/2} \quad (3)$$

As for the formula (3), ΔS_1, ΔS_2, ΔS_3 are the main three stresses of single axial. $\Delta\varepsilon_{eq}$ and the ΔS_{eq} obtained by the above equations will be used later in the Cycle stress-strain formula to find develop the Cyclic stress-strain curve.

2.3 Cyclic stress-strain relation and Plastic revision under Multi-axial loading.

An elastic-plastic material, which was subjected to cyclic loading will have the strain-stress history which will initially go through a transient state which asymptotes to a cyclic state. (Maksimovic, 2005). Additionally, the behaviour of body, within this cyclic state can be divided into three main region; Elastic region (recoverable deformation), Elastic-plastic region (permanent deformation) and lastly, Failure.

This cyclic-stress strain curve is particularly possible to be obtained by connecting the stable hysteresis loop's tips for different strain amplitude in a fully reversed strain-controlled test. However, tests for this purpose will not be conducted in this study due to the limitation of time and costs. The cyclic stress-strain curve will be obtained through calculation; utilising the Cyclic stress-strain formula (eq.4).

The basis of the cyclic stress-strain formula comes from the Ramber-Osgood equation. This equation (Ramber-Osgood equation) is basically the representation of multi-axial loading, stable cycle stress and strain curve in analytical form.

$$\Delta\varepsilon_{eq} = \Delta\varepsilon_{eq}^{e} + \Delta\varepsilon_{eq}^{p} = \frac{\Delta\sigma_{eq}}{E} + 2\left(\frac{\Delta\sigma_{eq}}{2K'}\right)^{\frac{1}{n'}} \qquad (4)$$

Both $\Delta\sigma_{eq}$, $\Delta\varepsilon_{eq}$ represent the equivalent range of local stress and strain in multi-axial loading; *E* is the Young's Modulus/Modulus of Elasticity, *n'* is the cyclic hardening exponent; *K'* is the cyclic strength coefficient, $\Delta\varepsilon_{eq}^{e}$ and $\Delta\varepsilon_{eq}^{p}$ are equivalent elastic and plastic stress range respectively. Maksimovic had utilized equation (4) along with the known material properties to define the cyclic stress-strain curve (figure 4) of the material tested. The curve also reflects the material behaviour towards cyclic loading.

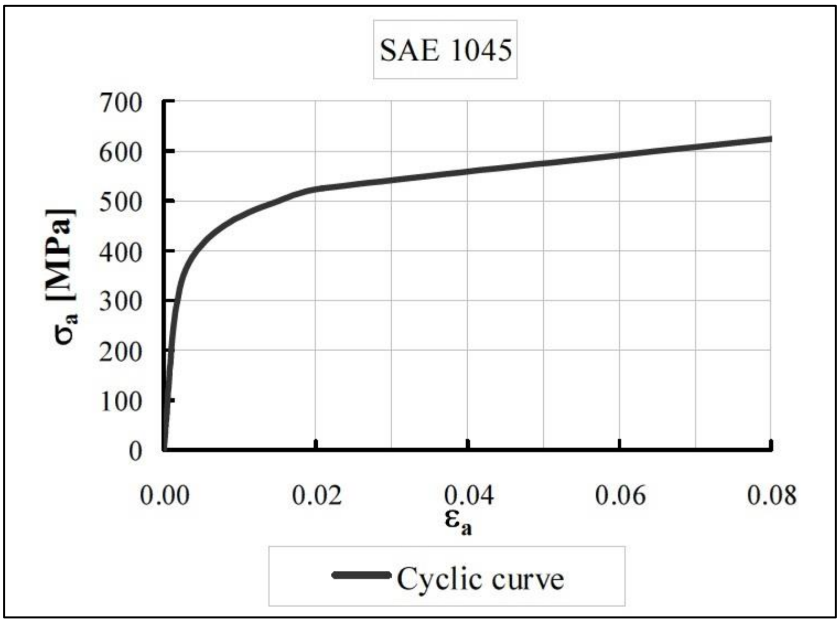

Figure 4: Cyclic stress-strain curve of SAE 1045 steel used in Maksimovic's *Fatigue Life Analysis of Aircraft Structural Component* research

2.4 Stress Analysis

Maksimovic (2005) had also mentioned in his paper: *Fatigue Life Analysis of Aircraft Structural Components*, stress analysis has two roles regarding to the fatigue life assessments. Firstly, to determine the area of component that is most susceptible to metal fatigue. Secondly, stress analysis is also important in providing means to overcome the localized nature of fatigue; that is to create alternative solution in preventing stress concentration and at the same time, reducing the risk of metal fatigue.

E. Vreudge of Metserve International (Metallurgical consultancy) had stated in his published Technical Brief literature (2001) that the stress concentration is one of the most significant factors that are affecting metal fatigue. Thereby, the understanding of importance of the stress concentration as one of the metal fatigue factor was already quite established. Not only that, it also had contributed a lot in the development of fatigue life prediction technique. Similar to what Maksimovic had done in his study, Teng & Chang (2003) have also used a simple plate with central hole model for their Finite Element (FE) analysis

In their study, Stress distribution determination was done through the Finite Element (FE) Analysis because of its capability in evaluating stresses reliably for complex geometries as well due its accuracy. Plasticity properties of the component at the stress concentrated area will be considered as well.

2.4.1 Finite Element Method

Alongside the analytical method (calculation), Finite Element (FE) method was utilised as well. FE Method was known for its accuracy in providing results through simulations. Other than known for its accuracy, Finite Element method has been a great tool to simulate operating conditions in terms of loading applications and predict how those loadings affects the structure; which will be the main focus in this study.

Below is the result of stress analysis through Finite Element done by Maksimovic (2005) in his study. The plot is colour coded where the highest magnitude of stress was represented by red and the lowest is represented by purple. From the Finite Element Analysis shown below, a pattern of stress distribution can be observed where the stress magnitude is the highest at the side of the hole of the plate, which indicates the stress concentration points.

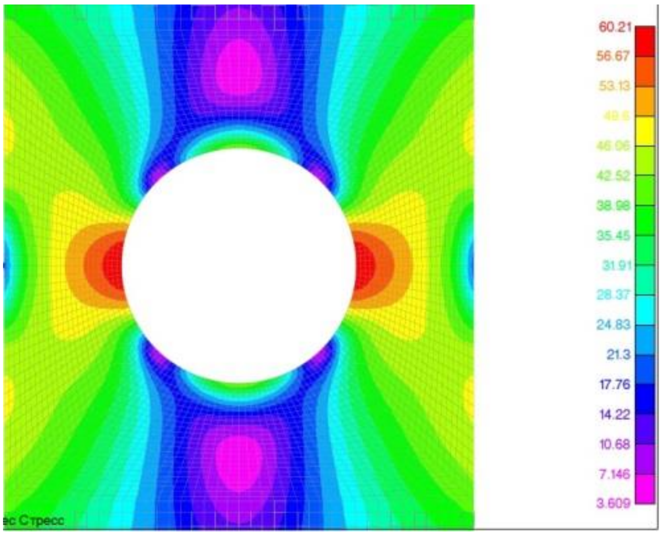

Figure 5: FE analysis on plate-with-hole in S. Maksimovic's paper; *Fatigue Life Analysis of Aircraft Structural Component.* (2005)

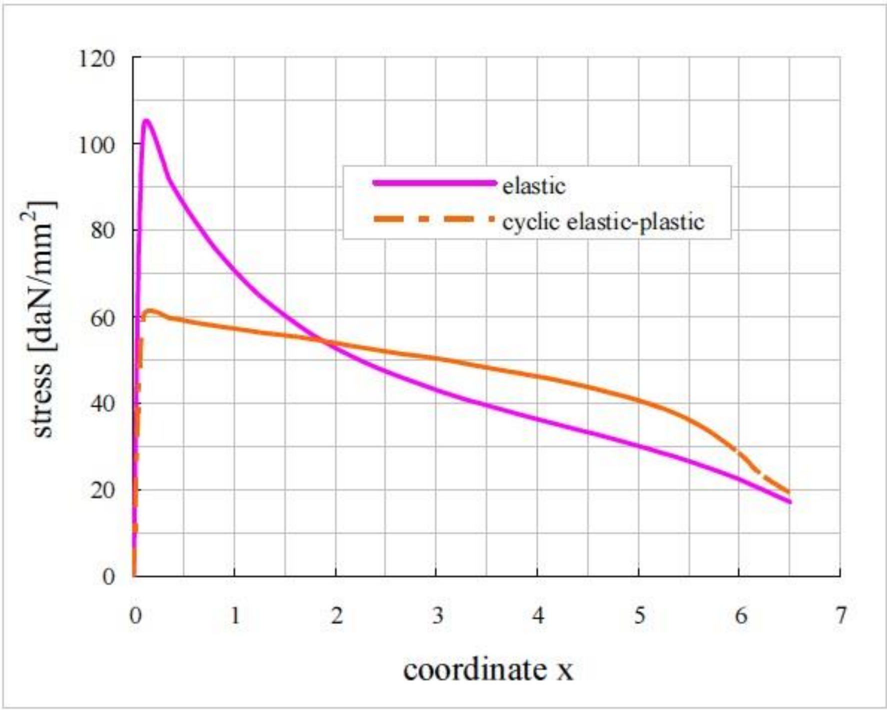

Figure 6: Stress distribution graph by x-axis coordinate in S. Maksimovic's paper; *Fatigue Life Analysis of Aircraft Structural Component.* (2005)

Adopting a little bit different way, Teng & Chang (2003) had used a symmetric representative model (a quarter of its holed plate) instead of using the whole plate-with-hole model. This had allow a very refined meshing on the part, which help the analysis to be highly accurate without having a very long time to solve the analysis. Below is the model representation used by Teng & Chang (2003) in their study and also their result after running the Finite Element (FE) solver for the stress analysis.

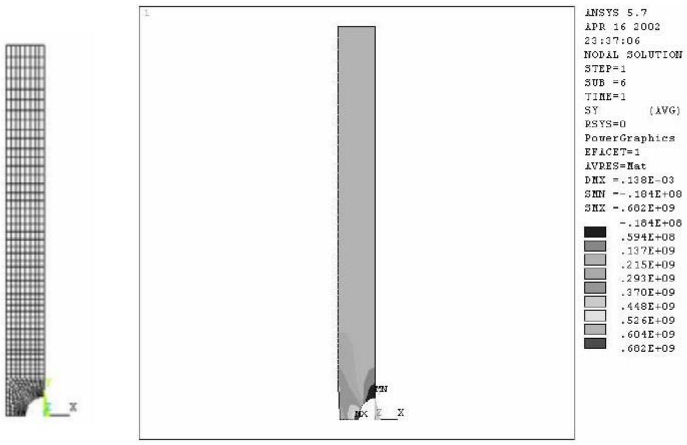

Figure 7: Model used by Teng & Chang (2003) for FE stress analysis

In determining the stresses and strains, non-linear (elastic-plastic) analysis was used and within this non-linear analysis, the cyclic curve of material behaviour was also used. The obtained value of local stresses was then used in fatigue life estimation.

2.4.2 Neuber's Rule

As loading is being applied to a notched structural component, the highly stressed part is localized around the notch root area. To compute the local stresses and strains at the localized stress area, Neuber's rule is used in conjunction with the cyclic stress-strain properties as well as Fatigue stress concentration factor. The Neuber's rule is as follows;

$$k_t = (k_\varepsilon k_\sigma)^{1/2} \qquad (5)$$

Where $\boldsymbol{k_t}$ is theoretical stress concentration factor, $k_\sigma \left(= \sigma / S\right)$ the local stress concentration factor and $k_\varepsilon (= \varepsilon / e)$ is the local strain concentration factor. Meanwhile, $\boldsymbol{\varepsilon}$ is local strain, $\boldsymbol{\sigma}$ is local stress, $\boldsymbol{e}$ is nominal strain and S is nominal stress. (Young, Budynas and Sadegh, 2012)

This relationship was then modified for the application of the fatigue loading (Topper, Wetzel and Morrow, 1969) by including the fatigue stress concentration factor along with the nominal stress range ΔS nominal strain range Δe, local stress range $\Delta\sigma$, local strain range $\Delta\varepsilon$ to become:

$$k_f (\Delta S \, \Delta e)^{1/2} = (\Delta\sigma \, \Delta\varepsilon)^{1/2} \qquad (6)$$

When the loads are too small that the material behaviour of the whole component is nominally elastic, then $\Delta S / \Delta e = E$ and equation (6) becomes:

$$\frac{k_f^2 \ \Delta S^2}{E} = \Delta\sigma \, \Delta\varepsilon \qquad \mathbf{(7)}$$

Since the left-hand side of the above equation was known for a given loading and geometry, this alternate form of Neuber's rule equation provides a relation in between $\Delta\sigma$ and $\Delta\varepsilon$ which are unknowns. Both of the local stress and strain ranges mentioned earlier are also related through the material stress-strain behaviour. These two relations; Neuber's rule and material stress-strain law determines $\Delta\sigma$ and $\Delta\varepsilon$.

$$\Delta\sigma = \frac{\Delta\sigma}{E} + 2\left(\frac{\Delta\sigma}{2K'}\right)^{1/n'} \quad (8)$$

Next, substitution of cyclic stress relation equation (8) into the equation (6) will give expression that relates local stress range to the applied nominal stress range and k_f hence through this, $\Delta\sigma$ could be solved.

$$(\Delta\sigma)^{1/2}\left[\frac{\Delta\sigma}{E} + 2\left(\frac{\Delta\sigma}{2K'}\right)^{1/n'}\right]^{1/2} = k_t(\Delta S)^{1/2}\left[\frac{\Delta S}{E} + 2\left(\frac{\Delta S}{2K'}\right)^{1/n'}\right]^{1/2} \quad (9)$$

The value of $\Delta\sigma$ will then substituted back in equation (8) to solve for $\Delta\varepsilon$. For the case of multi axial loading, equation (5) will need to be modified that all the stresses and strains need to be replaced with equivalent stresses and strains (look section 2.1).

Below is the modified equation:-

$$\Delta\sigma_{eq}\ \Delta\varepsilon_{eq} = \frac{k_t^2\ \Delta S_{eq}^2}{E} \quad (10)$$

2.5 Fatigue Life Analysis

Maksimovic (2005), in his paper had used strain based approach for the fatigue life estimation. In this approach, local stresses and strains at notches $\boldsymbol{\sigma}$ and $\boldsymbol{\varepsilon}$ were estimated and played a main role in determining fatigue life predictions. According to Rahman et. al. (2009), this kind of approach (strain-life approach) involved the techniques of converting the loading history, geometry and material properties (monotonic and cyclic) input to become fatigue life estimation. The analytical method of this approach was based on the low-cycle fatigue data in terms of strain-life curve and it (strain-life curve) was preferred to be used to present the strain cyclic resistance of materials by describing material's endurance as function for both elastic and plastic strain amplitude. Below is the equation which relates the applied strain range and fatigue life under multi-axial loading and this equation was known as Morrow equation.

$$\frac{\Delta\varepsilon_{eq}}{2} = \frac{\sigma'_f - \sigma_m}{E}\left(2N_f\right)^b + \varepsilon'_f\left(2N_f\right)^c \qquad (11)$$

In the previous equation, (equation 11) $\Delta\varepsilon_{eq}$ is the equivalent strain range; $\boldsymbol{b}$ is the Basqun's coefficient; $\boldsymbol{c}$ is the fatigue ductility exponent; σ'_f is Basquin's fatigue strength coefficient; and ε'_f is fatigue ductility coefficient and σ_m is the local mean stress.

2.6 Fatigue Cumulative Damage

The damage induced by metal fatigue is accumulative in nature. The damage may have been started during the early days of its usage and under the repetitive loadings that may be well below the yield point. This process is particularly dangerous because a single load application would not show any apparent ill-effect. (Roylance, 2001). So, to estimate the fatigue damage under a spectrum of variable amplitude of repetitive loading, Palmgren-Miner rule was used. Maksimovic (2005) had adopted this law in his paper as well to estimate the fatigue damage due to variable amplitude of cyclic loading which represents the load that aircraft structure/components have to bear during its life.

Miner law equation is as follows;

$$D = \sum_i \frac{n_i}{N_{fi}} \qquad (14)$$

Where, $\boldsymbol{D}$ represents the damage due to fatigue, $\boldsymbol{N_{fi}}$ is the cycle count at the time of failure under axial loading and $\boldsymbol{n_i}$ is the actual cycle count at the adequate stress level. However, to suit the strain-life approach of fatigue life estimation, the above equation (14) will be expressed as follows;

$$T = \frac{1}{\sum_i \frac{n_i}{N_{fi}}} \qquad (15)$$

Where $\boldsymbol{T}$ is the block load spectrum during structure failure.

The block load spectrum concept has been used in Maksimovic's had considered both constant and variable amplitude of loading in order to increase the accuracy and realism (compared to constant amplitude loading application) and at the same time reduces the complication of the real time history (variable amplitude loading) the of the cyclic stress application upon the investigated aircraft structure during flight (Fatemi, 2009).

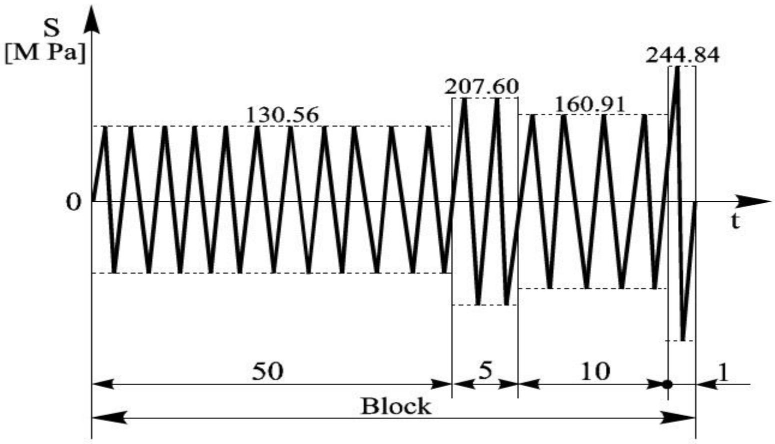

Figure 8: Block load spectrum used in Maksimovic's paper; *Fatigue Life Analysis of Aircraft Structural Component.* (2005)

Table 1: Block load cycles used in Maksimovic's paper; *Fatigue Life Analysis of Aircraft Structural Component.* (2005)

				Nfi [cycles]		Nbl	
No.	ni	Pmax [kN]	Smax [MPa]	Analytical solution	FEM	Analytical solution	FEM
1.	50	25.27	130.56	$0.21399\ 10^5$	$0.37459\ 10^5$		
2.	5	40.18	207.60	$0.22140\ 10^4$	$0.19216\ 10^4$		
3.	10	31.14	160.91	$0.67311\ 10^4$	$0.95469\ 10^4$		
4.	1	47.39	244.84	$0.11901\ 10^4$	$0.61964\ 10^3$	$0.14449\ 10^3$	$0.151278\ 10^3$

The above examples of the block load spectrum and block load cycles are from Maksimovic's result data. The block load spectrum example in the figure 8 represents the cycles of loading encountered by an aircraft in ONE typical flight cycle and the following table 1 had shown the number of block load spectrums (Nbl) or simply put; the number of flight cycles before crack initiation would begin in the tested model of holed aircraft component.

3. METHODOLOGY

3.1 Analysis Tool

3.1.1 ANSYS Workbench 15.0.7 software

ANSYS Workbench software is one of several Finite Element-capable softwares that are vastly used in many kinds of applications. In short, like any other finite element software, this software is capable of conducting simulations and analysis in various principles of engineering such as the structural analysis (involving stress, deformation, etc.), computational fluid dynamics (CFD), heat transfer analysis, and many more.

Like most of the finite element analysis software, the mechanism of this software in conducting analysis generally is the same like any other FE analysis software. A model need to be generated first either using the built-in design media or through other design software which later, can be imported into this software for analysis. Next, the model will undergoes through the process of meshing, where the whole area of the component will be divided into nodes to increase the accuracy of the analysis and the number of these nodes can be adjusted. Technically, the higher number of nodes, the smaller the mesh will be and the more accurate the analysis result will be. However, it will take a longer time to finish due to the increased number of nodes to be analysed. The opposite will happen when the number of nodes is fewer. The simulation's solver will take into consideration all the governing equations and theorems related to the analysed topics. Upon the completion of the analysis, numerous types of results can be displayed to determine the maxima and the minima for any properties. The result will be displayed in the form of color-coded contour upon the surface of the 3D model. Typically, red will be the maxima of the investigated properties and dark blue will be the minima of the investigated property.

Meanwhile, this research had been using this software mainly to determine the maximum stress magnitudes under several loading conditions and also its localization points within the tested virtual model. This research had also been using this software to determine the number of lives upon certain magnitude of forces (which analogous to forces of flight loading spectra). The solver embedded within the software will be utilising all the governing equations presented earlier in the literature review part using all the predetermined properties of material and conditions of loading. Data gathered from the finite element analysis were then being used to calculate the total number of flight load spectra (which represents the flight cycles). The final calculated load spectra will be the final result and will then be validated by comparing the result of this study to the previous research works.

3.1.2 CATIA V5 software

This Computer Aided Drawing (CAD) software is very common in engineering field as design software and due to its user-friendliness, engineers and designers preferred this software in producing complex and intricate components, regardless of how small or how big it is. Users are allowed to create 2D and 3D sketches and from those sketches, it can be imported to any types of softwares for any types of applications. For example, a CAD drawing made from this software can be imported to ANSYS (FE analysis software) for FE simulation or to any Computer Aided Manufacturing (CAM) software for manufacturing processes. Due to this flexibility, CATIA has been one of the highly regarded CAD software available in the industry. In fact, this software had also been used intensively in the design process of Formula 1 cars (Dassault Systems, 2001) and also in the design of Boeing's technologically advanced and successful aircraft, the Boeing 777 series (Boeing, 2015).

As for this study, CATIA V5 software is the software of choice for this study as a tool to produce the virtual model (plate-with-hole) which then be tested in the finite element analysis through the ANSYS Workbench software. The model to be made from this software will be in the form of 3D model instead of 2D in order to give a 360-degree view of stress effects towards the virtual model produced while being simulated under flight condition in FE analysis and hence will help to improve the understanding of stress concentration effect towards fatigue life of the holed aircraft component.

3.2 Project Activity

In this research project, research activities were planned accordingly in order to ensure that all the research procedures and steps were executed properly and in being done in orderly manner. Before all the exact project work could be initiated, thorough and deep research had been done upon the topics that are related to the study such as metal fatigue, aircraft structures, loading characteristics, flight envelope and etc. Research was done through a lot of media which includes internet, research journals, research papers, journal articles, text books, and many more. This is particularly important to ensure that the topics related to the study can be thoroughly understood hence could prevent/reduce the errors or misinterpretation of results as the study progresses. Additionally, the thorough understanding of the topic could also be helpful in providing some ideas during this study to improve the current and previous practices, research works or methods either to make the overall process simpler or even to help in producing a better and more accurate result through the improved method.

Next, the project reaches the second phase which is the analysis model determination process. After having an extensive research through literatures regarding this topic, the analysis model was then being determined and the main criteria that it needs to fulfil is to be able to represent as close as possible the characteristics of common holed structures/components that exists in aircraft. As mentioned earlier in the literature review part, this study will employ the local stress-strain concept which permits the usage of the simpler-shaped model to be used in the analysis as it is sufficiently representative to the real complex-shaped model. In this study, rectangular plate-with-hole model has been chosen as it is simple and practical to be used for analysis and it had also been used in the previous research works as well due to the same reason, simplicity and practicality. During this phase, the material of the model had also been decided. The model had been assigned with the properties of AISI 1045 (medium carbon steel). The main reason for this material to be chosen for the model is mainly for the validation process. Previous researches had used AISI 1045 as their assigned material. In order to validate this project's result to theirs, it is important for us to use the same material, under the same loading condition so that the comparison will be valid.

After that, the project activity continued with the Finite Element (FE) analysis through the ANSYS software. In this phase, the produced model will be simulated under several loading magnitudes and then under an approximated typical flight loading condition. The simulation which applies several magnitudes of loading is mainly to determine the localization point of the stress when it is applied to the model. Then, the model was simulated under cyclic loading condition in order to observe the effect of stress concentration in the form of hole to the life cycle of the component. After the effect was observed, another simulation was done the model. This time, the simulation will be replicating the approximated typical flight condition. The model will be imposed to several magnitudes of forces under several cycles. These magnitudes of forces under several cycles can also be described as block load spectrum which also known generally as flight cycles. At this part of simulation, the life cycles of the model under the exposure of different magnitudes of cyclic loading will be determined. All of these simulations had utilized all of the governing equations and theories which were explained previously in the literature review part.

As all of the life cycles of the model under the exposure of different magnitudes of cyclic loading were determined, modified version of Miner's Law equation was used to determine the number of block load spectra that the component might survive before the fatigue crack initiation occur. In this phase, normal calculation will be done by applying the formula in determining the total block load spectra. The final result obtained will be compared to the result from the previous research which utilizes different but established method by calculating the percentage of error. This comparison is important for the validation purposes of the obtained result hence determine whether the technique is accurate and reliable enough to be used in the industry as well as in research field.

Finally, once the method had been validated and proven to be accurate and reliable to be used, it will be applied as a case example onto a real holed-aircraft component from a real aircraft (Zenith air CH601XL model). In this simulation, the part, which is in the form of 3D model, will be simulated under the typical flight conditions using the same method used earlier to a simple plate-with-hole model. Stress localization will be observed and the effect of the stress concentration upon the life of the model will be determined. Additionally, the overall block load spectra (flight cycles) that the aircraft component will able to withstand before the crack initiation process will be determined as well using the method established earlier (tested earlier upon plate-with-hole model).

3.1 Analysis Work

This study will be applying several rules and theorem for both of the stress analysis as well as the fatigue analysis. It is to be noted that the analysis were being done through ANSYS finite element (FE) software and all of the governing equations, rules and theorem were already embedded in the software and being used as solvers. Below are the procedures of the analysis applied in this study;

1. All of the loading conditions and the material properties were pre-determined. The loading condition will mimics the typical condition during the whole flight cycle which will be encountered an aircraft. The loading condition will be used as the load-time history for the fatigue simulation.

2. Then, the Von Misses criterion was applied for the stress analysis and taking the Elastic-plastic revision as well into consideration. Through the simulation, the whole data of stress localization (concentration) point and stress maxima/minima were obtained. It is to be noted that the loading applied in this simulation is cyclic loading.

3. After that, the study proceeded with the fatigue analysis. During this analysis, a fatigue simulation which utilizes the strain-life method was carried out. All the governing equation related to strain-life method was used in the simulation as a solver along with several specified loadings. This particular simulation is to see the effect of stress concentrations upon the fatigue life of the model. The simulation was repeated using the same stain-life method of fatigue analysis with complete parameters of typical flight loading condition

4. The fatigue simulation was repeated using the same stain-life method of fatigue analysis with complete parameters of typical flight loading condition. By the end, the accumulation of damage due to fatigue damage will be summed linearly using Miner's rule by taking into account the number of block load spectra that the component will endure before the fatigue crack initiation start to occur.

3.3 Project activities flowchart

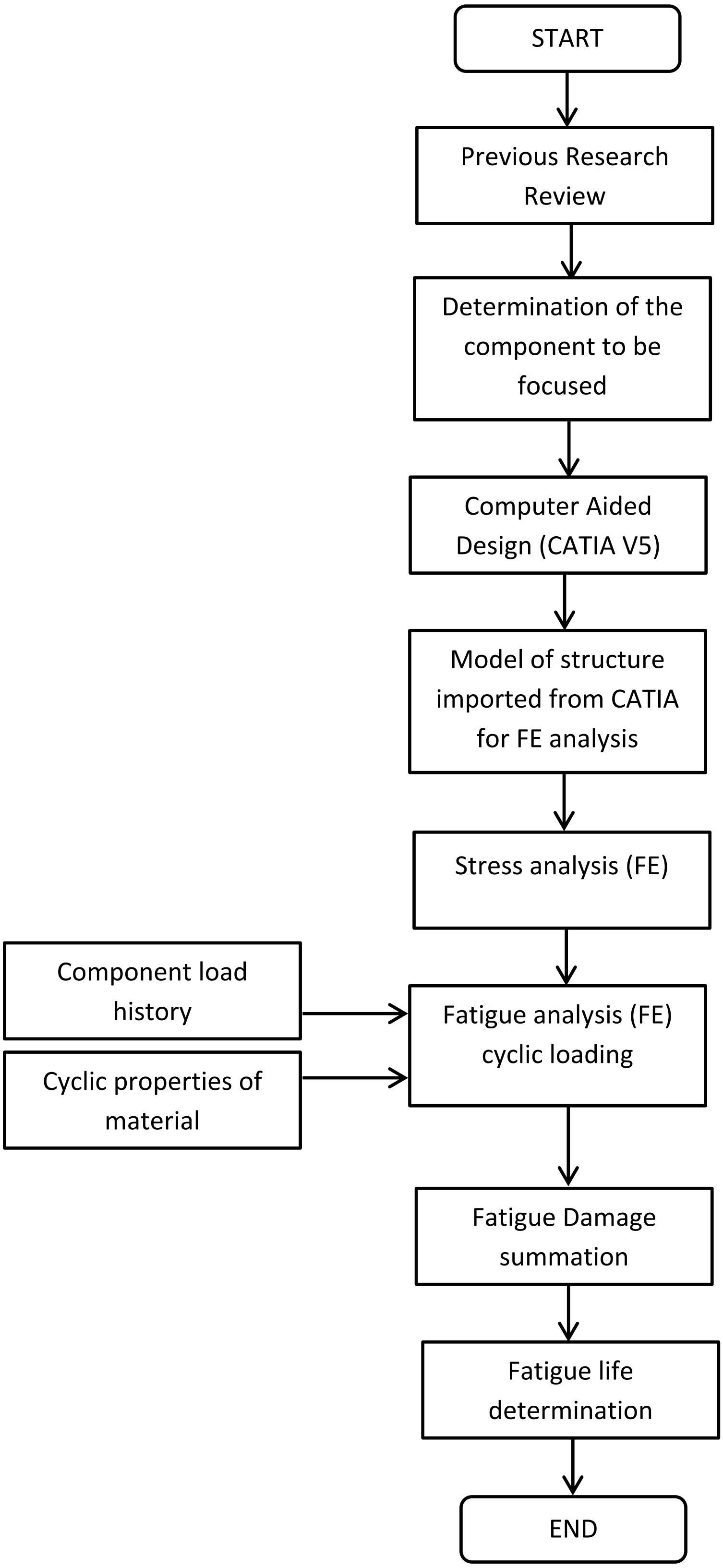

3.4 Gantt Chart (FYP 1) and Project Milestones

Project activities	WEEK NUMBER													
	1	2	3	4	5	6	7	8	9	10	11	12	13	14
Selection of project topic (proposed by lecturers)	■	■												
Research work commenced - Look for references, resources - Study the literatures - Prepare extended proposal		■	■	■	■									
Submission of Extended Proposal						★								
Preparation for proposal defense - Rework and refine proposal - Further look for references - Preparing materials for proposal defense							■							
Proposal Defense								■	■					
Research work continuation - Further look for references - Identify room of improvements of the proposed project procedures - Prepare Interim report										■	■	■		
Submission of Interim Report draft													★	
Corrections for Interim Report draft													■	
Submission of final Interim Report														★

3.5 Gantt Chart (FYP 2) and Project Milestones

Project activities	WEEK NUMBER														
	1	2	3	4	5	6	7	8	9	10	11	12	13	14	15
Commencement of project work - Creating CAD model for the FEA simulation															
Stress-strain analysis - Utilizing FEA to conduct analysis - Obtaining stress-strain information; (curves, data to be used in fatigue analysis) - Preparation of Progress Report															
Submission of Progress Report															
Fatigue Analysis and Pre-SEDEX preparation - Conducting fatigue analysis using strain-life method - Using fatigue crack initiation method to predict fatigue life - Using Miner's Rule to sum up fatigue damage accumulation -Preparation for Pre-SEDEX															
Pre-Sedex															
Preparation of Final Report															
Submission of Draft Final Report															

Submission of Dissertation (soft bound) and Technical Paper												★			
Viva													★		
Submission of Final Project Dissertation (hard Bound)															★

Legend:

- marked the process

★ - marked the Project milestone

4. RESULTS AND DISCUSSION

4.1 Stress Analysis

As discussed in earlier section, in order to see the localization of stress (stress concentration) on a component/part, stress analysis need to be carried out. In this experiment, a stress analysis was carried out upon a simple virtual model of plate-with-hole through Finite Element (FE) method. The material chosen for the model is AISI 1045 (Medium strength steel). Below are the 3D model’s dimensions and its material characteristics and properties;

3D Plate-with-hole Model Dimensions

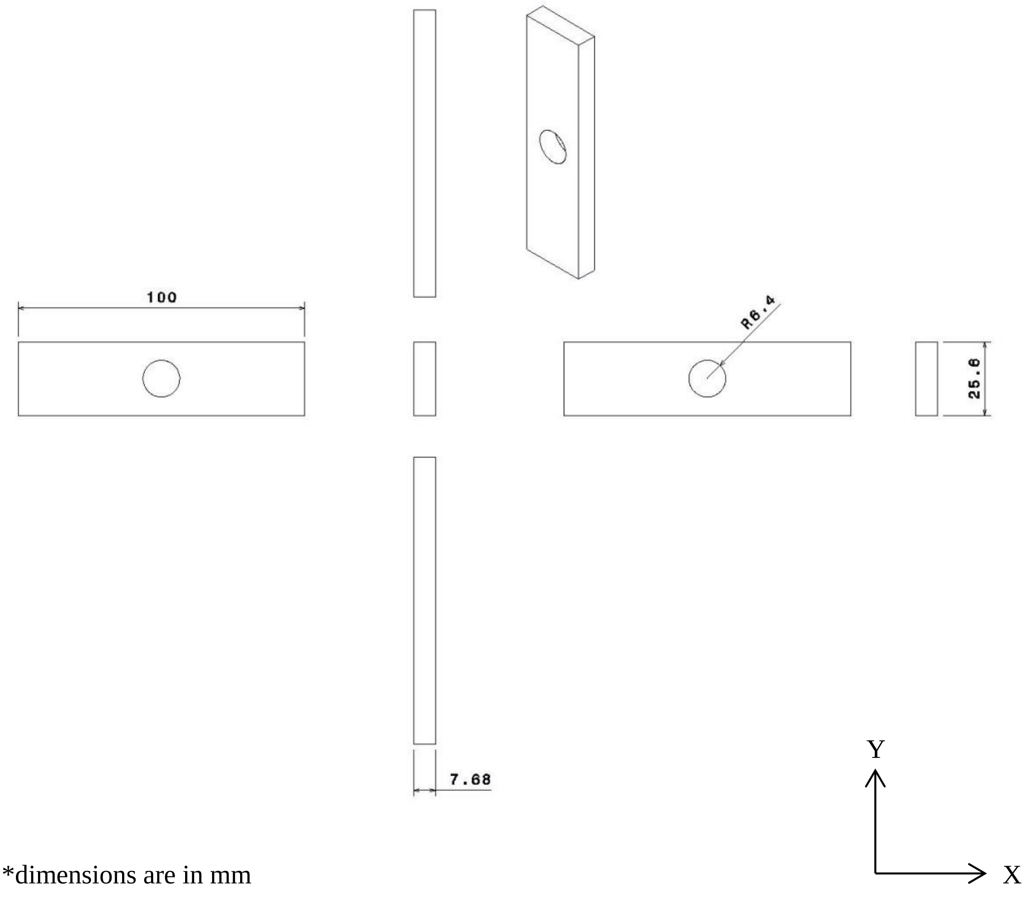

*dimensions are in mm

Properties of AISI 1045 steel

Table 2: Physical and mechanical properties of AISI 1045 steel

Physical Properties	Metric	Imperial
Density	7.87 g/cc	0.284 lb/in^3
Mechanical Properties	**Metric**	**Imperial**
Hardness, Brinell	163	163
Hardness, Knoop (Converted from Brinell hardness)	184	184
Hardness, Rockwell B (Converted from Brinell hardness)	84	84
Hardness, Vickers (Converted from Brinell hardness)	170	170
Tensile Strength, Ultimate	565 MPa	81900 psi
Tensile Strength, Yield	310 MPa	45000 psi
Elongation at Break (in 50 mm)	16.0 %	16.0 %
Reduction of Area	40.0 %	40.0 %
Modulus of Elasticity (Typical for steel)	200 GPa	29000 ksi
Bulk Modulus (Typical for steel)	140 GPa	20300 ksi
Poissons Ratio (Typical For Steel)	0.290	0.290
Shear Modulus (Typical for steel)	80 GPa	11600 ksi

Getting back to the stress analysis, the simulation was done by applying 40.18kN of tensile load on both ends of the plate and the body was left unconstrained, making sure that the only force that are reacting to the body is literally just the tensile forces acting on both ends of the plate.

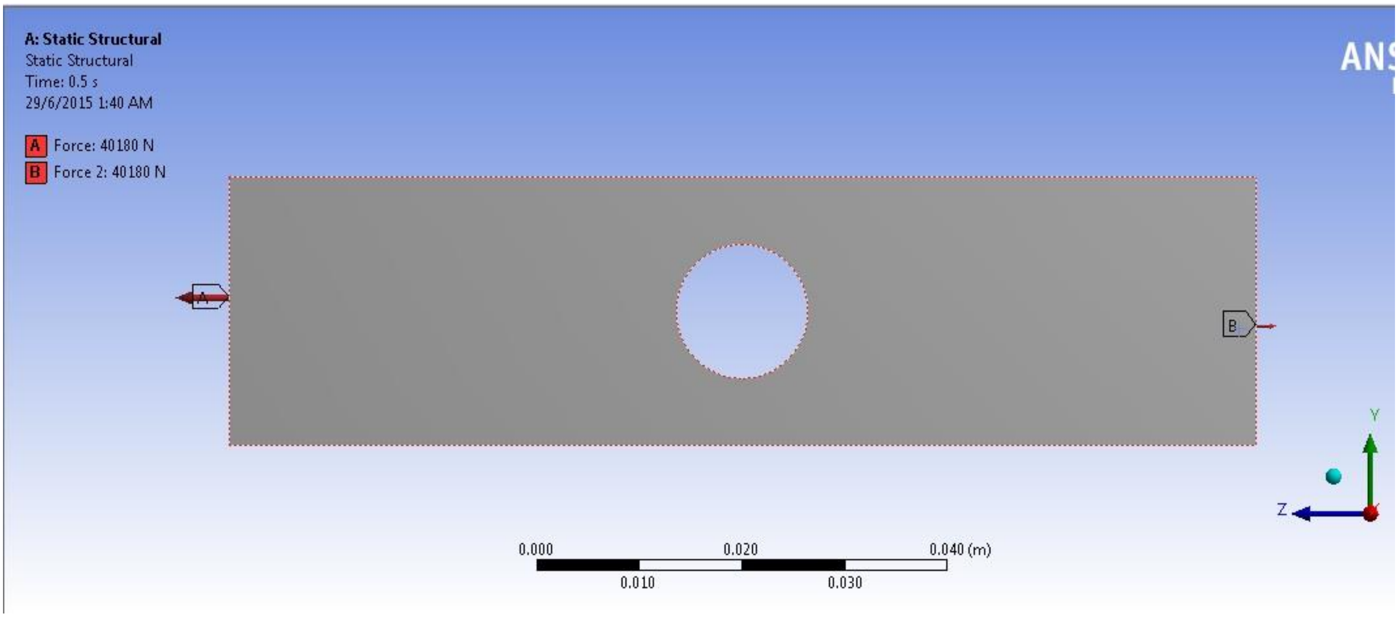

Figure 9: Direction and magnitude of forces applied to the plate

Both of the forces at this time are not yet cyclic loadings but instead, both of them are just static loadings. This stress analysis will not take into account any fatigue effect upon the model as it is simply to look upon the stress localization point when loading is applied to the plate-with-hole model. It is to be noted that the Von-Mises criterion discussed earlier in the previous part (literature review) had also been considered for this stress analysis. The following figure 10 shows the colour-coded contour of stress intensity and the magnitude of stress when 40.18kN of force applied to the model.

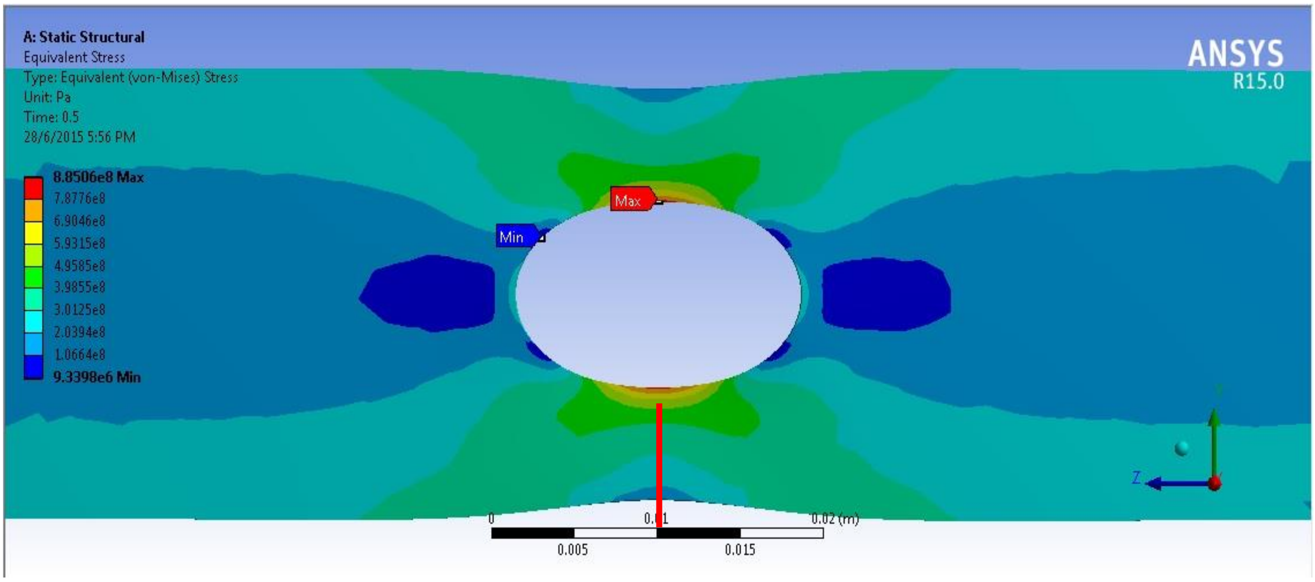

Figure 10: Stress distribution contour for load application of 40.18kN

In the above figure, red represents the maximum magnitude of equivalent stress (Von Mises stress) and the darker tone blue represents the minimum magnitude of equivalent stress. From the result of this stress simulation, it can be seen that the highest equivalent stress magnitude happened to be at the upper part of the hole in the Y-axis direction with the magnitude of 885.06 MPa and lowest equivalent stress magnitude happened to be at the upper-left side of the hole with the magnitude of 9.3398 MPa. From the obtained result too, it can be seen that the stress is mainly concentrated from the upper and lower-middle part of the plate up to the upper and lower hole. Below is the stress-distribution graph along the co-ordinate marked red in Figure 11.

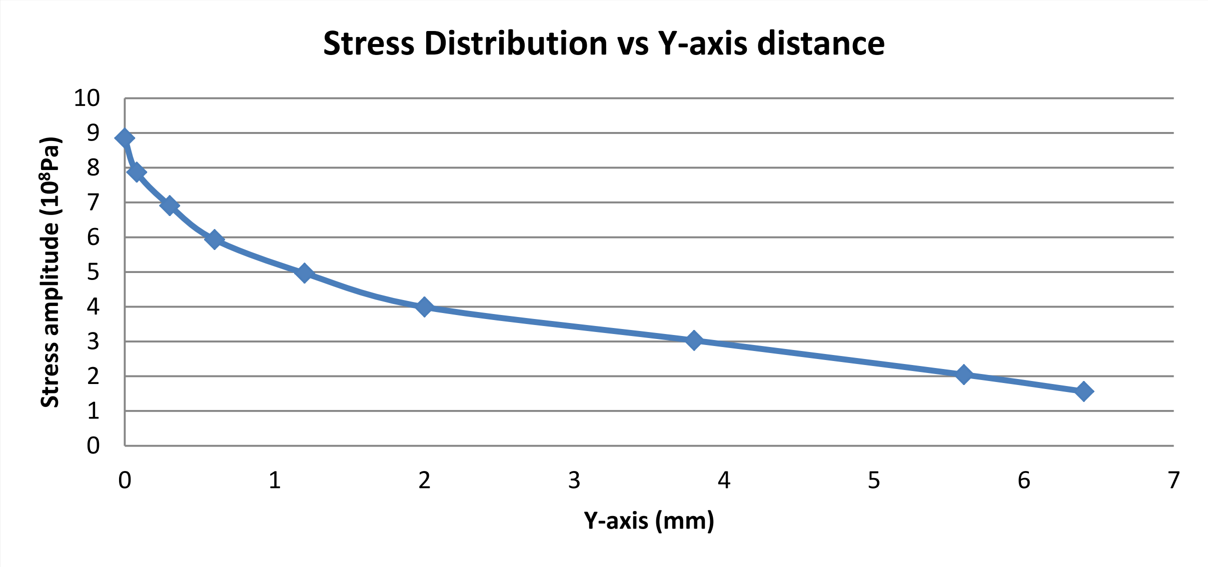

Figure 11: Stress distribution graph on red-marked part of the plate

In the above graph, the position 0 of Y-axis starts at the hole and the rest is continuous up until the side of the plate. Through the graph presented in figure 11, it can be observed that at the position Y=0, which is at the lower part of the hole (within the red line) has the highest stress magnitude and it decrease gradually as the position gets further from the hole. It was also known that at position Y=0, the magnitude of stress is about 6 times higher than the magnitude at edge of the plate, giving a clear indication of stress concentration at the upper and lower area of the hole.

From all the observations made from this analysis, it can be determined that the localization of stress do occur at the upper and lower area of the hole as the magnitude of stress is very high at that region. In fact, about 6 times higher that at the edge, and about 95 times higher than the minimum stress observed (at the right and left hand sides of the hole). This proves the point made earlier that the presence of hole in a geometry/part can be a stress raiser or concentrator when load is applied to the geometry/part. Hole is part of discontinuities that may exist within parts, structures and materials. Whenever there are discontinuities, there will be stress localization to occur when it is exposed to loadings. This is almost likely the same case as the presence of microvoids within a metal due to the manufacturing defects. Same like the hole present in the tested plate, these microvoids will be the point at which stresses will be concentrated at. Since the stress magnitude is so immensely high within the stress concentration point, it has been predicted that the crack initiation might occur at the location which the stress is maximum within the tested plate. It was also predicted that the percentage of damage will be highest at the aforementioned stress concentration region if cyclic loadings were to be applied to the plate. To confirm this prediction, the fatigue life analysis was carried out and the results were presented and discussed in the next part of the report.

4.2 Fatigue life Analysis

Fatigue life analysis had been carried out in this study by considering the usage of cyclic loading upon the plate-with-hole model in the simulation. This analysis was divided into two parts in which the first one, a simulation was done by applying only one particular magnitude of cyclic loading to the plate-with-hole model to see the effect of stress concentration upon the fatigue life of the tested model. Meanwhile, the second part of fatigue analysis was done by applying several magnitudes of loading profile which mimics a typical flight loading condition for a conventional aircraft. Both of the simulations had considered the strain-life method of fatigue life analysis and had applied Morrow equation to determine the fatigue life of the tested model. However, since the second simulation had considered several magnitudes of forces within a loading spectra, modified version of Miner's rule had been utilized to sum linearly all the damages (in terms of life cycle count) that occur to the plate-with-hole model and this summation will be done manually without any finite element (FE) software application. Several characteristics of the AISI 1045 under cyclic loading that are particularly useful for the fatigue life analysis were also applied. Below are the material characteristics of AISI 1045 under cyclic loading.

Fatigue strength exponent, b	-0.081
Fatigue ductility exponent, c	-0.67
Fatigue strength coefficient, $\sigma`_f$	1165.6 MPa
Fatigue ductility coefficient $\varepsilon`_f$	1.142
Modulus of Elasticity, E	2.069×10^5 MPa
Cyclic strain hardening exponent, n`	0.123
Cyclic strength coefficient, K`	1062.3 MPa
Cyclic Yield Strength, S_y	648.3 MPa
Cyclic Ultimate Strength, S_u	786.2 MPa

Through the usage of equation (4) as presented in the literature review part, a cyclic stress-strain curve was obtained. The obtained cyclic stress-strain curve shows the strain reaction of the material upon the application of increasing magnitude of cyclic stress to the AISI 1045 Medium Strength steel.

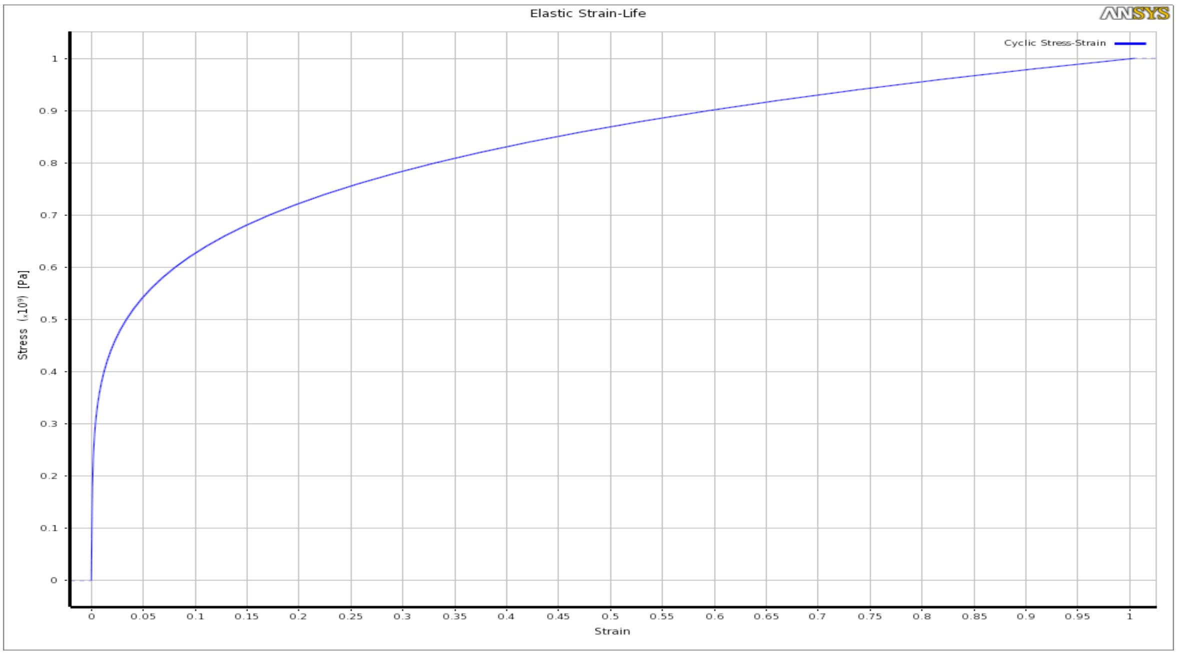

Figure 12: Cyclic stress-strain curve of AISI 1045

The above cyclic stress-strain curve is particularly important in process of fatigue life estimation for any material especially when the analysis is being done through manual analytical method. As the case for this study, the information from the cyclic stress-strain curve is very important for the solver of the finite element software to carry out the fatigue life estimation. This cyclic stress-strain curve can be considered as the properties of the AISI 1045 because it is unique to AISI 1045 when the cyclic loading with increasing amplitude applied onto it.

4.2.1 Stress concentration-fatigue life relationship

As mentioned earlier, this first part of fatigue analysis will only be considering a magnitude of cyclic loading (40.18kN). The loading will be applied to the model in tension parallel to Z-axis (refer figure 9). The following figure 13 shows the life cycle at particular points of the plate-with-hole model component as the cyclic loading of 40.18kN was applied.

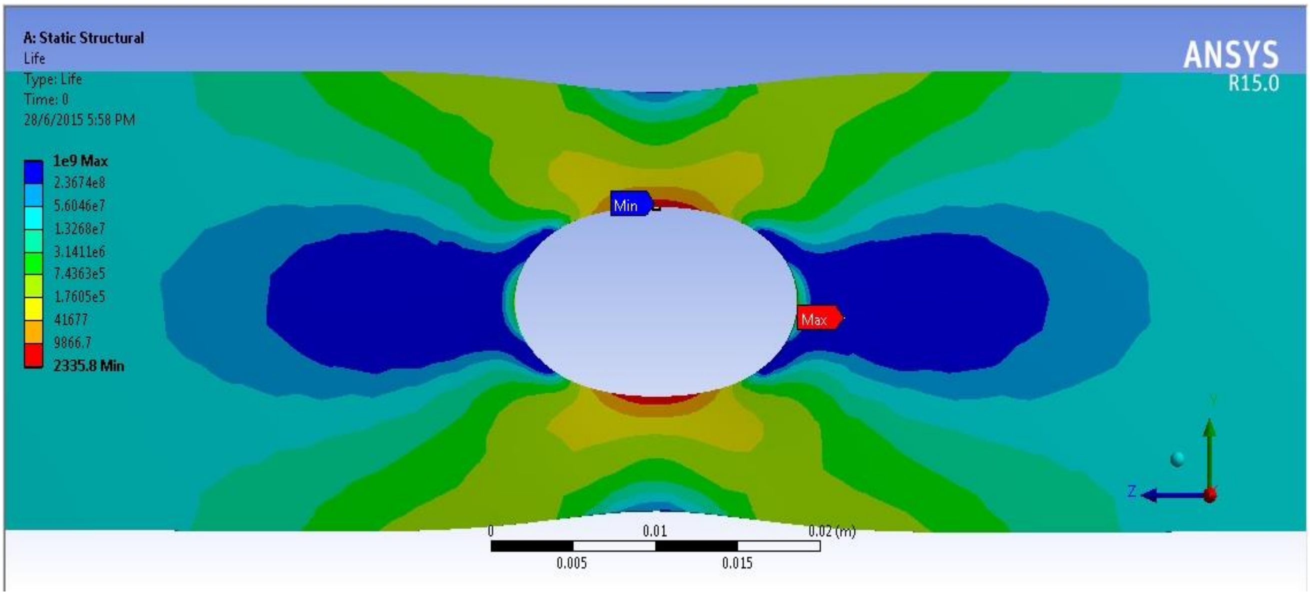

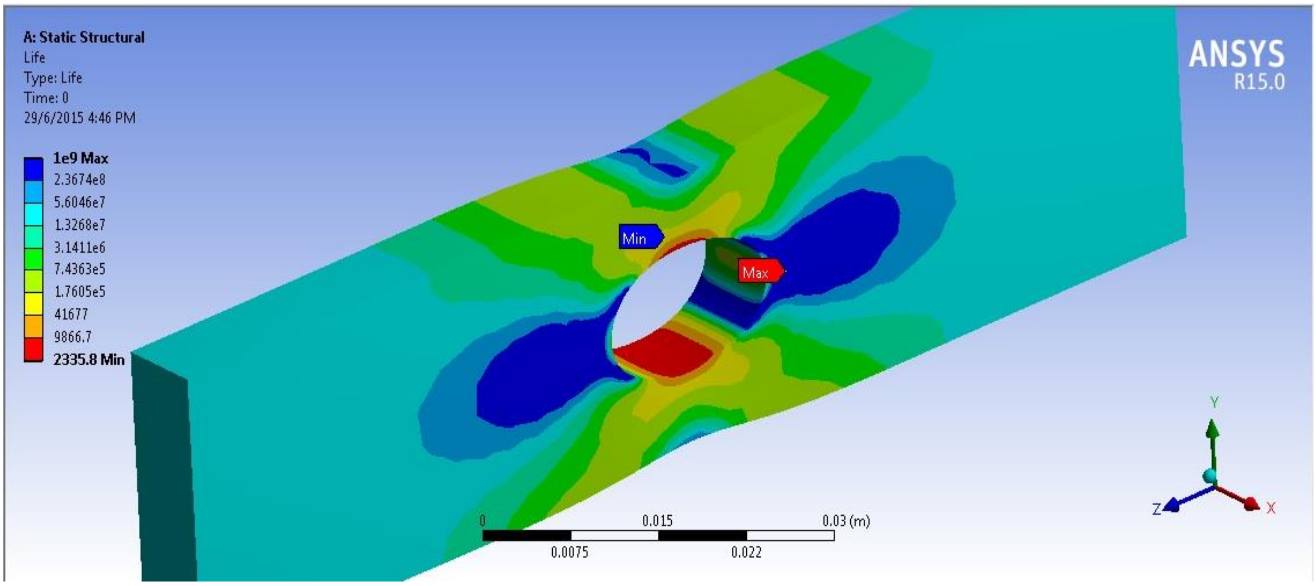

Figure 13: Distribution of life cycle within the model of plate-with-hole under cyclic loading of 40.18kN

In the above figure, the contour plot is practically almost the same as the contour plot seen in the stress analysis. However, the difference in this plot is this time, blue represents the highest magnitude of life cycle (showing indication of less damage severity) and red represents the lowest magnitude of life cycle (showing indication of high damage severity). As far as the fatigue analysis was concerned, the life cycle distribution pattern that is almost the same as the stress distribution pattern from the previous simulation can be seen. The location where in the previous analysis the stress is concentrated is also the location at which the life cycle is lower. Meanwhile, the location of the life cycle is the lowest deviates a little bit as compared to the lowest stress magnitude location from the stress analysis result but it is still within the low magnitude of stress region in the tested model. In this fatigue analysis, it was found out that the lowest magnitude of life cycle is 2335.8 cycles, and the highest magnitude of life cycle is $1x10^9$ cycles.

Relating from the information of the stress concentration location obtained from the stress analysis and the information of life cycle distribution from this fatigue analysis simulation, some obvious similarities can be seen. As mentioned earlier, the stress and life cycle distribution pattern is almost the same where the location of the life cycle is the lowest at the place where the stress magnitude is the highest. This indicates that the location at which the stress is maximum/life cycle is the lowest has sustained the worst damage among other location in the model. The fact that the loading applied to the specimen is the cyclic type of loading, it had made the damage even worse at the location at which the stress is the highest. The location at which the life cycle is the lowest is place where the fatigue crack will start to initiate. D. Roylance (2001) had mentioned in his paper that fatigue crack initiation begins at an internal or surface flaw where the stresses are concentrated and consists initially of shear flow along slip planes. Over a number of cycles, this slip generates intrusions and extrusions that begin to resemble a crack. In the case of this study, the flaw mentioned earlier is practically can be referred to the hole at the plate. Hole itself is a discontinuity that exists on the plate and as cycles of force continues to be applied upon the model, slip bands started to occur which eventually creates intrusions and extrusions at microscopic level. As the cyclic forces continued to be applied further, these intrusions and extrusions will eventually initiate fatigue crack.

All in all, it can be concluded from this first fatigue analysis simulation that the stress localization which occur at the lower and upper part of the hole of the model had caused that particular location to have a multiple times lower fatigue life as compared to the other part of the model. It was also agreed that the aforementioned location on the model is the place where the fatigue crack will start to initiate as it will sustain the most damage during the period of cyclic loading application.

4.2.2 Fatigue life estimation of model under typical flight loading condition

In this second part of fatigue analysis, the fatigue life of the plate-with-hole model was estimated through the same method used earlier. However, in this part, a typical flight loading condition was applied to the model where there were several different magnitudes of loading associated instead of only one and the analysis was done mostly through finite element (FE) method and the final damage summation part was done manually using a formula derived from Miner's rule. The obtained fatigue life estimation was be compared to Maksimovic's result for validation purpose. Below is the block load spectrum which was used in this simulation

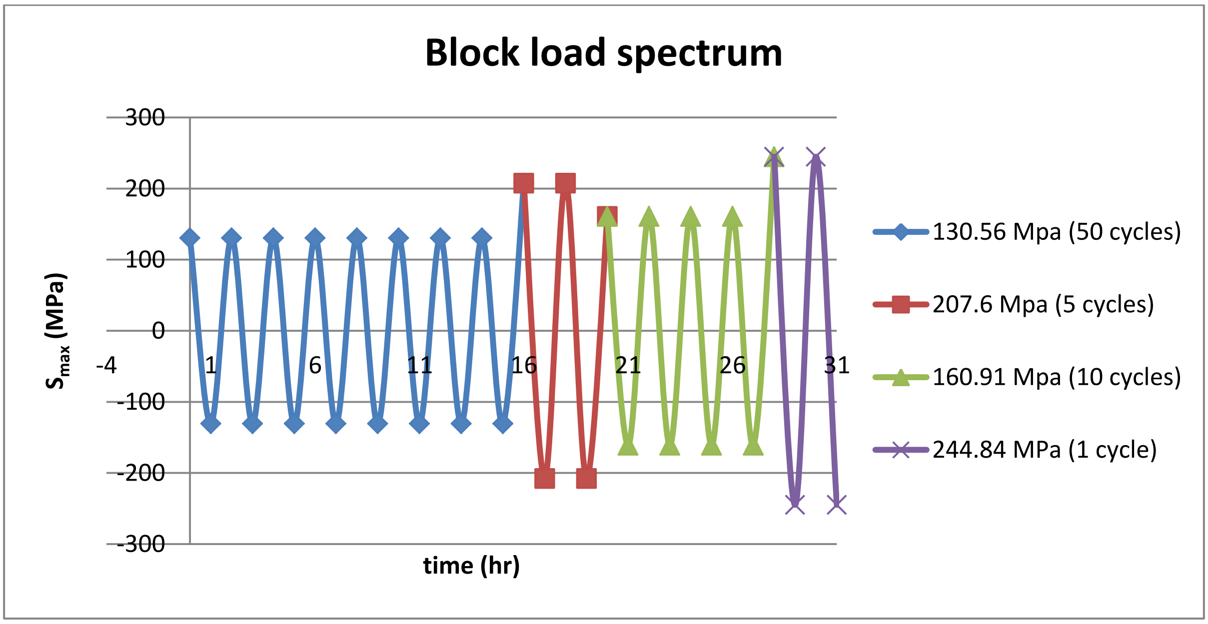

Figure 14: Block load spectrum used in the fatigue simulation

Note that the block spectrum used in this simulation is the same block load used by Maksimovic in his paper shown in Table 1. The use of the same block load spectrum is important for the validation purposes as the result obtained from this simulation was compared to Maksimovic's. The percentage of error between the result from this simulation and Maksimovic's will be the tool for validation. It is to be noted as well that the S_{max} shown in the above block load spectrum was calculated normally through simple formula of Tensile Force applied ÷ Cross sectional area.

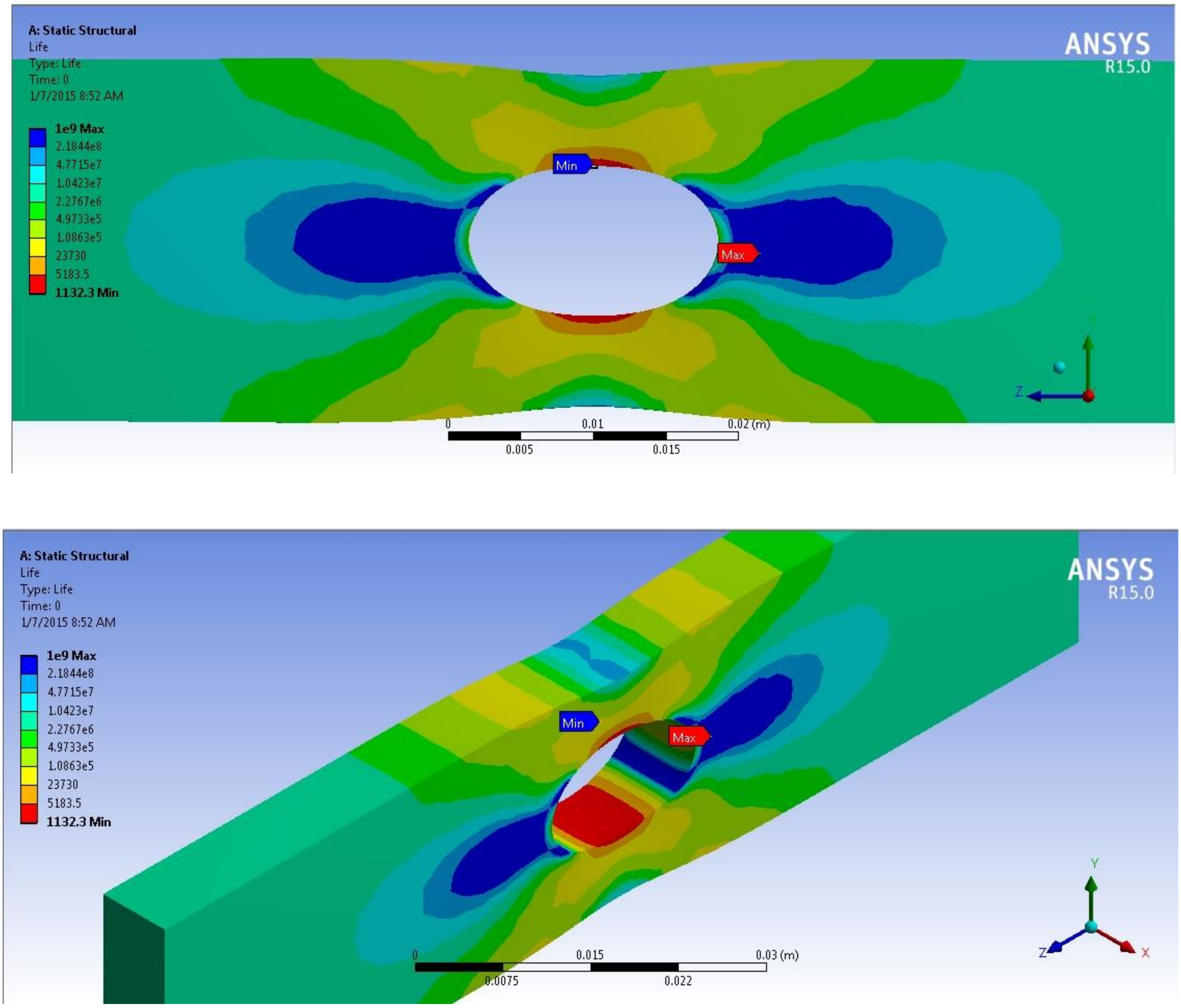

Figure 15: Distribution of life cycle, $\mathbf{N_{fi}}$ within the model of plate-with-hole under cyclic loading of 47.39kN ($\mathbf{S_{max}}$ = 244.84 MPa)

Table 3: Number of cycles up to crack initiation for plate with central hole (take R=-1)

No.	Actual cycle count, **ni**	Load, **P** (kN)	$\mathbf{S_{max}}$ (MPa)	Cycle count at time of failure, $\mathbf{N_{fi}}$	Number of block spectra up to crack initiation, $\mathbf{N_{bl}}$
1	50	25.57	130.56	22404	
2	5	40.18	207.60	2335.8	
3	10	31.14	160.91	7697.6	
4	1	47.39	244.84	1132.3	152.55

Percentage of Error evaluation

Maksimovic's N_{bl} = 151.28

Obtained N_{bl} = 152.55

$$\frac{152.55 - 151.28}{151.28} \text{x}100 = 0.84\%$$

Error = 0.84%

From the obtained result of the second fatigue simulation, it can be observed that all of the life cycle, N_{fi} distribution pattern for all 4 magnitudes of forces have that the same pattern where the location at which the minimum life for the model will be at the lower and upper middle part of the hole. The only differences that can be seen when all 4 magnitudes of forces being applied to the model is the resulting number of minimum life cycle. The higher the force applied, the lower the minimum life cycle at failure will be.

After having all the Cycle count at time of failure, $\mathbf{N_{fi}}$ linearly summarized using equation (15), the final Number of block spectra up to crack initiation, $\mathbf{N_{bl}}$ (which represents the number of Flight Cycles (FC)) obtained is 152.55. This means that, when the model is being exposed to the typical flight loading condition (as shown in figure 14), it will take about 152 flights to have a fatigue crack to be initiated at the model. This result was also compared to Maksimovic's final result of his estimation from his research paper, *Fatigue Life Analysis of Aircraft Structural Component*. The percentage of error obtained is only 0.84%, hence it is confirmed that the simple method developed in this research study is valid and can be applied generally to determine the fatigue life of holed aircraft component.

By today's standard of aircraft safety, fatigue crack initiation at only 152 flight cycles (as obtained from the simulation) is actually very small. Fortunately, this is only a simple model where there are no safety factors and refinement of design being considered to increase the fatigue life of the aircraft component. An aircraft component will usually be designed to have an adequate safety factor and also designed to have a significant reduction of stress concentration which in turn, will help tremendously in increasing the fatigue life of that part. In aviation industry, it is also a normal practice for an aircraft to be inspected as frequently as possible and all of these inspections are very effective in managing the fatigue occurrences in aircraft components before catastrophic failure may even occur.

4.3 Application of the developed method to the example of the actual aircraft structure. (Wing rib #7, Zenair CH601XL light aircraft)

As shown in the previous part of the report, the method to estimate the fatigue life of an aircraft structure developed in this study have shown a quite promising potential as it had achieved about 99.16% of accuracy (0.84% error) as compared to the fatigue life estimation made in previous Maksimovic's study work. In this part, the method developed will be applied to determine the fatigue life of an actual aircraft structure. The part that has been chosen for this purpose is the #7 wing rib of Zenair CH601XL light aircraft.

Figure 16: Zenair CH601XL aircraft

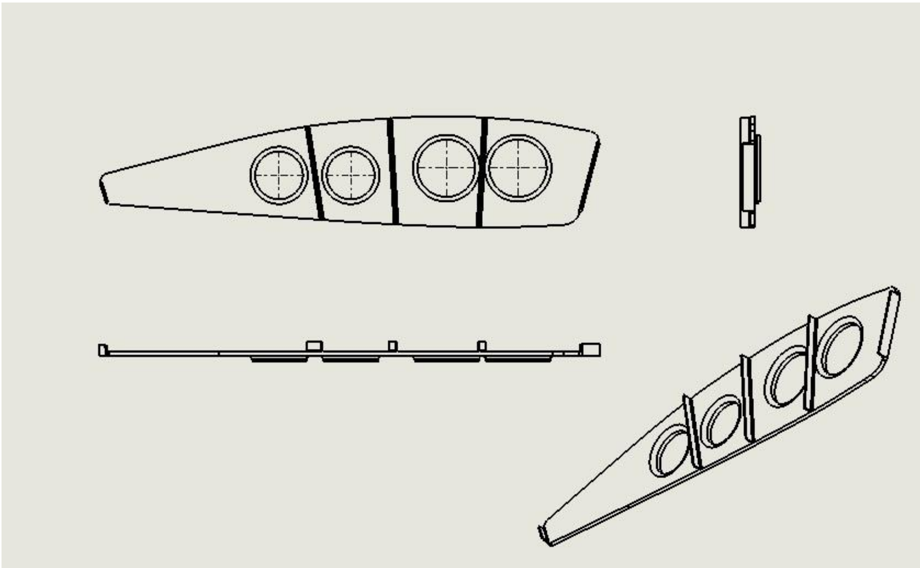

Figure 17: #7 Wing rib of Zenair CH601XL

As what had been done earlier with the plate with hole model, a simplified CAD model of the wing rib was produced using CATIA V5 software and was tested through ANSYS R15 finite element software using the predetermined parameters and properties. A theoretical flight loading spectrum was used in this fatigue life estimation process to simulate the loading that the component (#7 wing rib) might have theoretically encountered in its life. Additionally, the loading spectrum created had taken the actual aircraft's flight envelope (featured in Appendix part) and performance into consideration. Below is the theoretical flight loading spectrum applied to the wing rib.

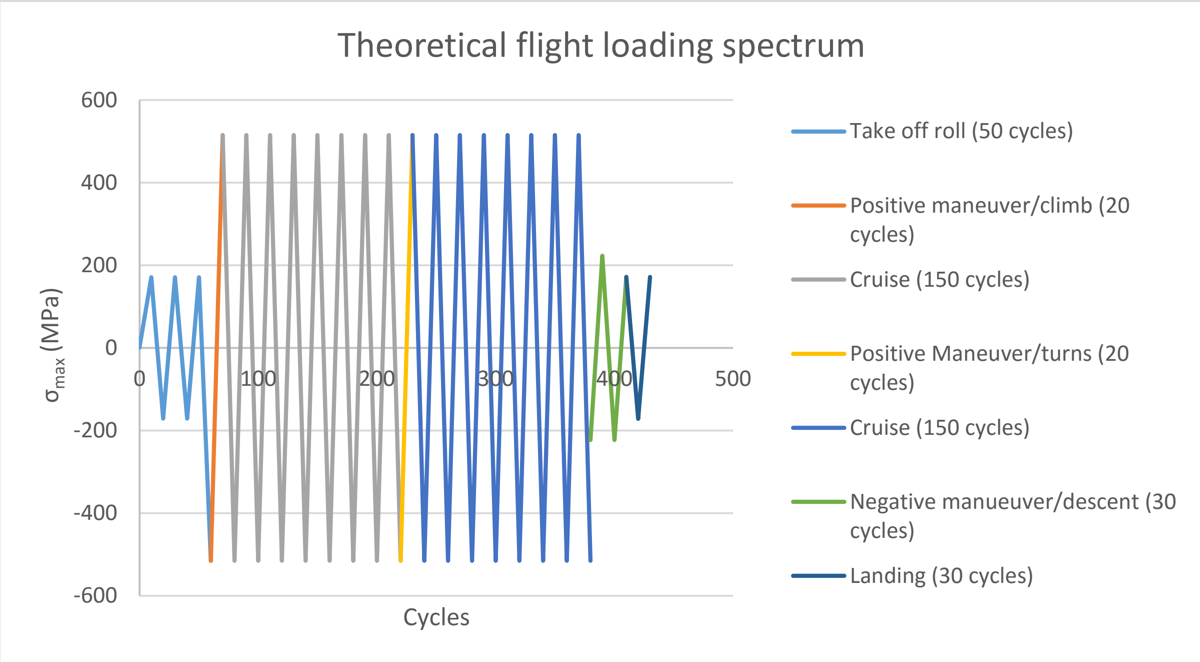

Figure 18: Theoretical flight loading spectrum

Like previously shown in the simulation using the plate with hole, stress analysis need to be done first before the fatigue analysis could be done to determine the maximum stress (σ_{max}) which will be needed in fatigue analysis to estimate the fatigue life of the part (wing rib). Meanwhile, the loading involved in this simulation is mainly **Lift** generated and **Weight** of the aircraft. Since both of these forces acted simultaneously and opposite to each other towards the component, only net force will be considered for the load application. Commonly, Lift and Weight was represented in terms of ratio, which is known as load factor, n

$$\frac{Lift, L}{Weight, W} = load\ factor, n$$

Load factor can be used to determine the lift generated by the wings at the particular attitude of the aircraft at given airspeed. On the other hand, the weight of the aircraft which was considered here is the **gross weight**, which is the weight where the aircraft will carry maximum amount of load that it could carry. The information of the aircraft performance and specifications were obtained through the data provided by the manufacturer in their public portal (presented in the appendix). The figure below shows the specific points at which the load is being applied to the wing rib. Note that only nett force (Lift - Weight) will be considered in this simulation.

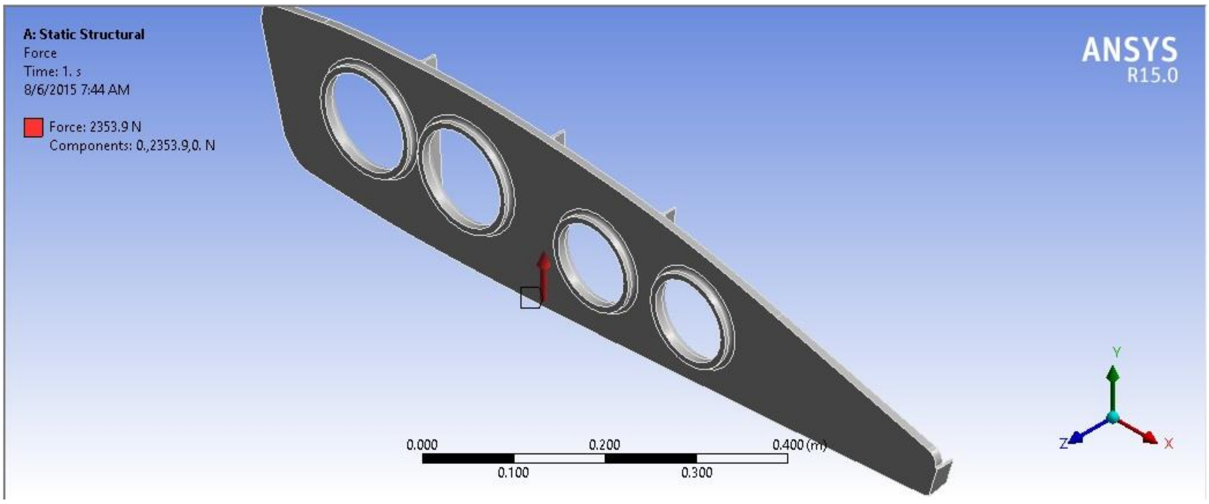

Figure 19: Application of load (view A)

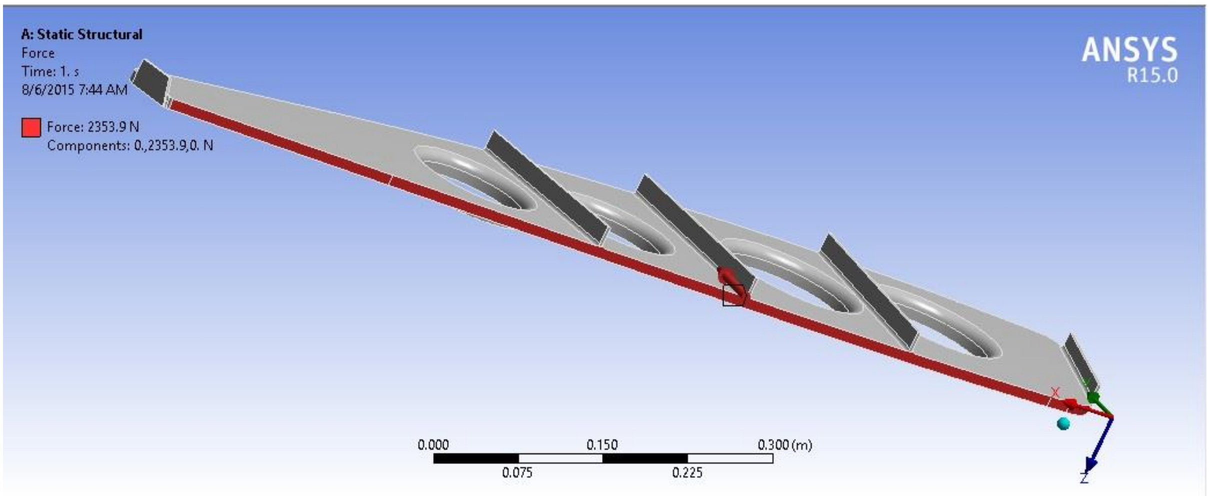

Figure 20: Application of load (view B)

It can be seen from the figure above that the application of load will only be at the underside of the wing rib, where both lift and weight acted upon it. Next, stress analysis were done for every magnitude of loading shown in figure 18 through the finite analysis software to determine the maximum stress, σ_{max}. As mentioned earlier, σ_{max} is one of the important information needed to make an estimation of the fatigue life through the developed method.

The figure below shows the point at which stress is being concentrated at the wing rib when one of the magnitude (Take off roll, 171.73MPa) of the static load is being applied to it. It is to be noted that the stress analysis was done at every magnitude of load within the theoretical load spectrum.

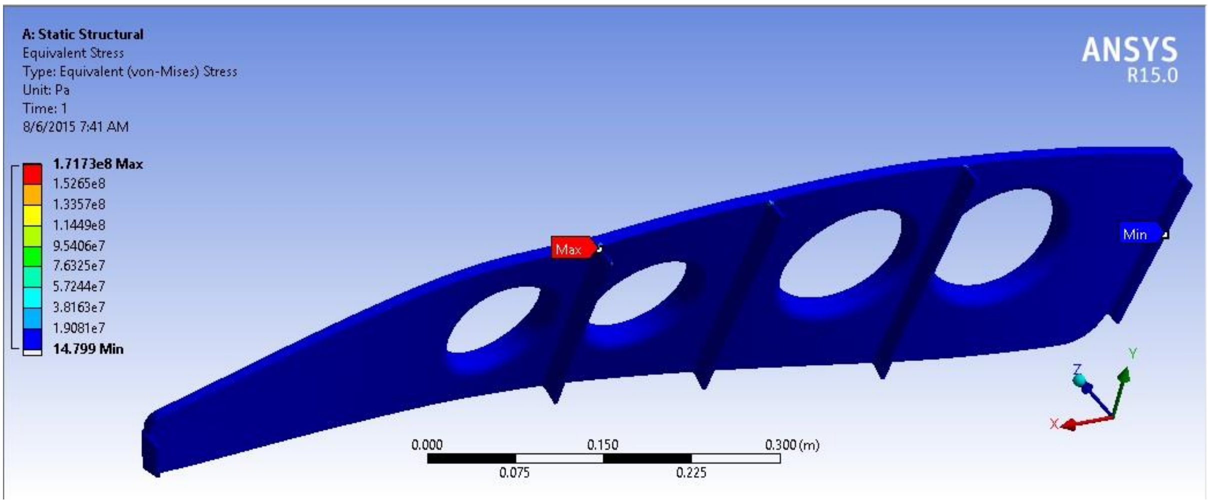

Figure 21: Stress distribution throughout the wing rib during take-off roll

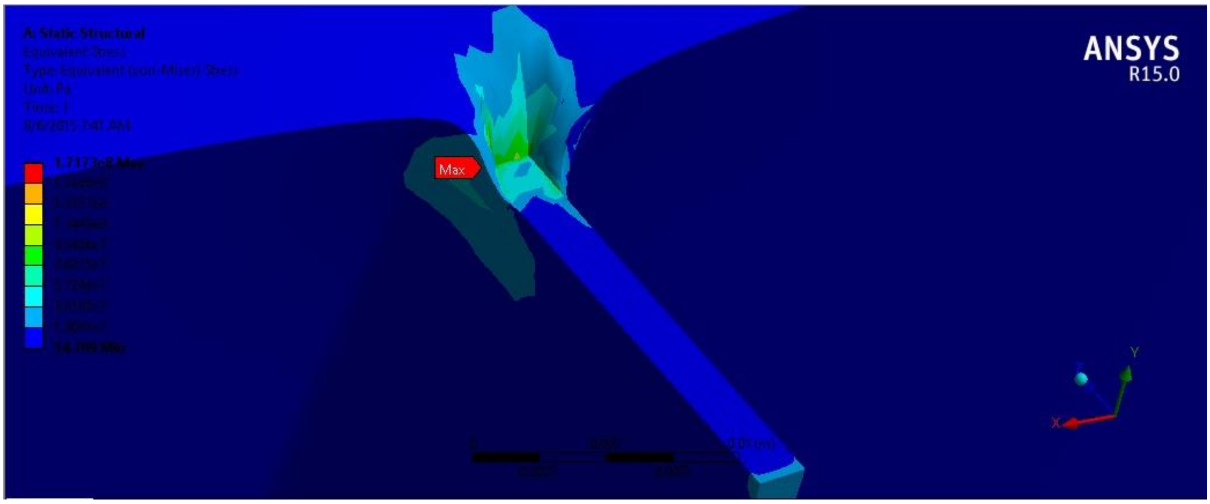

Figure 22: Stress distribution throughout the wing rib during take-off roll (zoom in)

Based on the above figures, it can be seen that the stress is mainly concentrated at the connection in between the main body of the wing rib and also the fin at which the wing skin of the aircraft will be attached to. The maximum magnitude of stress is mainly concentrated at the connection in between the rib's main body and the aft (#3) fin.

Next, the process continued with the fatigue analysis which utilizes the theoretical flight loading spectrum shown above as the loading history. At this point, all of the material data and also the cyclic properties of the material were plugged in to the software where the solver will carry out the calculation for the fatigue life estimation. In this particular simulation, strain-life method had been used and Morrow's equation had been utilized as the equation for the finite element solver.

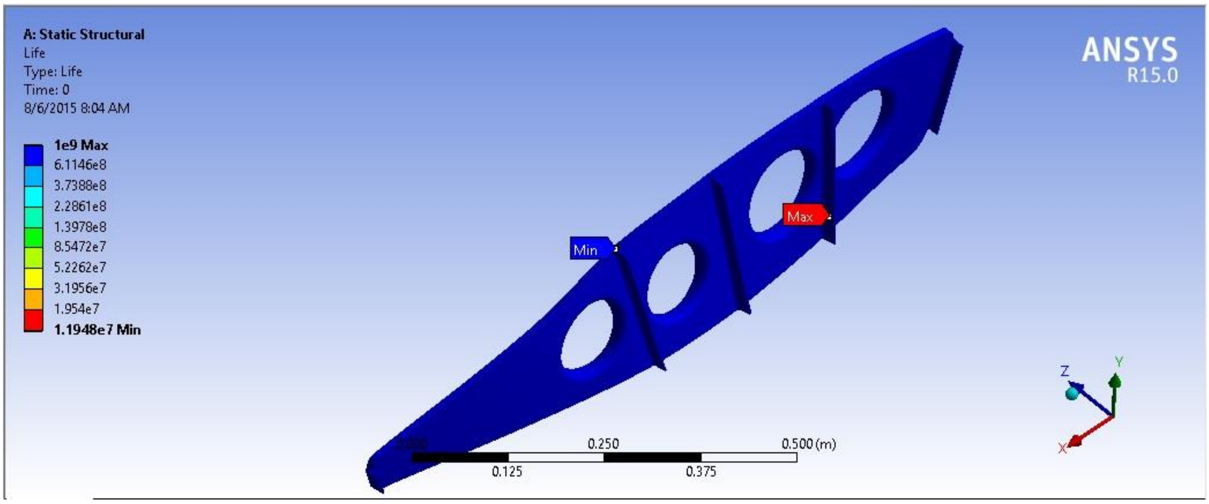

Figure 23: Fatigue life distribution contour for loading magnitude of 223.17 MPa

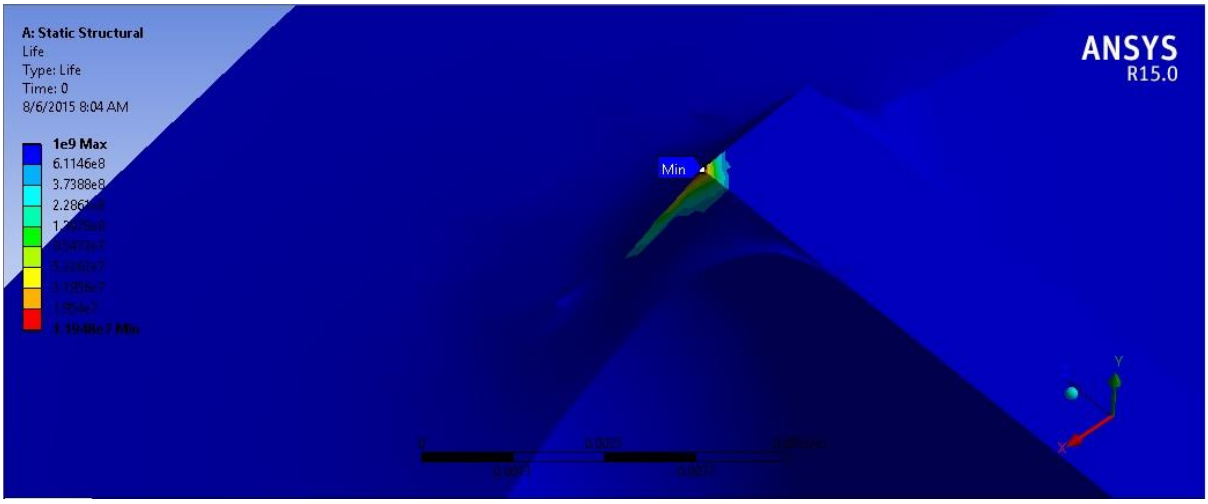

Figure 23: Fatigue life distribution contour for loading magnitude of 223.17 MPa (zoom in)

Consistent with the test done with the plate with hole model, it can be seen that the point at which the stress is the highest (stress concentration) has the lowest life cycle (N_{fi}) throughout the wing rib structure. The fatigue simulation was repeatedly done for all the magnitude of loading within the loading spectrum. Next, when all of the minimum life cycles were determined for every magnitude of loading, all of them will be summed linearly using the modified Miner's Law equation (equation 15) shown in the literature review part. The final value obtained is the Number of block spectra up until the crack initiation, N_{bl} or simply known as the flight cycle.

Table 4: Number of cycles up to crack initiation for wing rib model (take R=-1)

No	Actual cycle count, ni	Load, P (kN)	σ_{max} (MPa)	Cycle count at the time of failure, N_{fi}	Number of block spectra up to crack initation, N_{bl}
1.	50	2353.9	171.73	1.1603×10^8	
2.	20	7059.3	515.02	34240	
3.	150	7059.3	515.02	34240	
4.	20	7059.3	515.02	34240	
5.	150	7059.3	515.02	34240	
6.	30	-3059.1	223.17	1.1948×10^7	
7.	30	2353.9	171.73	1.1603×10^8	100.67

After having all the lowest life cycle summed, it was estimated that the first crack will start to initiate at the 100.67 flight cycle; which is after 100 flights. Additionally, from the information gained from the stress and fatigue life contour, it was also predicted that the crack will start to appear at the point of connection in between the main body of the wing rib as well as the #3 (aft) fin of the rib as the simulation had shown that the highest magnitude of stress (stress concentration) and the lowest life cycle count occur at that particular area.

5. CONCLUSION AND RECOMMENDATION

In conclusion, this study has been focusing on the development of simple and reliable fatigue life prediction procedure by using the strain-life approach and also the fatigue crack initiation method. In developing the procedure, an intensive usage of finite element (FE) software as well as Computer Aided Design (CAD) software was applied along as means to get accurate results easier and in a much shorter time than conducting experiments and full scale simulations. In the end, it was confirmed that the method developed in this study is generally valid to be used as a simple and reliable tool to estimate the fatigue life of an aircraft structure.

Additionally, this study had also focused on the effect of stress concentrators; which is in our case is hole within the aircraft structures to its fatigue life. Simulations were done to determine the stress concentration location and its effect towards the fatigue life of the component. It was found out that the stress concentration occur at the upper and lower part of the hole as tensile force was applied to the sample at Z axis (refer figure 9). It was also found out that the part with high stress concentration will have a significantly lower fatigue life which consistent with the assumption made before the simulation.

It is highly recommended that the method developed in this study to be applied in the industry as well as in the design analysis works as it could tremendously reduce the needs of full-fledge fatigue simulation and experiment which will consume a lot of money and also a lot of man hours. It is also highly recommended for further study work regarding this method to be done in order to improve this fatigue life estimation method and help making the method developed in this study to be more accurate and more suitable to determine the fatigue life of components in any kind of fatigue loading conditions.

REFERENCES

[1] ASME Code Case N-47-23 (1988). *Case of SME Boiler and Pressure Vessel Code,* American Society of Mechanical Engineer.

[2] Boeing (2015). *Computing & Design/Build Process Help Develop The 777: CATIA Development.* Retrieved on February 21, 2015 from: www.boeing.com/boeing/commercial/777Family/compute/compute4.page.

[3] Boeing 737-400 Structure Repair Manual (2012). Subject 53-00-07, *Chapter 53: Fuselage*, p.202 & 203.

[4] Boeing 737-400 Structure Repair Manual (2012). Subject 53-80-07 (Fuselage Frame), *Chapter 53: Fuselage*, p.204

[5] Dassault Systems (2001). *Formula One Teams Race on CATIA and ENOVIA Product Lifecycle Management Solution*. Retrieved on February 19, 2015 from www.3ds.com/press-releases/single/formula-one-teams-race-on-catia-and-enovia-product-lifecycle-management-solutions/.

[6] Fatemi, A. (2010) *Chapter 10: Multiaxial stress*, University of Toledo, Toledo, Ohio, U.S.A.

[7] Fatemi, A. (2009) Chapter 9: *Fatigue from Variable Amplitude Loading*, University of Toledo, Ohio, U.S.A.

[8] Findlay, S.J. & Harrison N.D. (2002). *Why Aircraft Fail?*, materialstoday, November 2002 edition, p.18-25

[9] Gautam, A. & Ajit, K.P. (2013). *Static Stress Analysis of Connecting Rod Using Finite Element Approach*, IOSR Journal of Mechanical & Civil Engineering (IOSR-JMCE), Volume 10, Issue 1, p.47-51.

[10] Husin, Z., Rahman, M.M., Kadirgama, K., Noor, M.M., & Bakar, A.R. (2010). *Prediction of Fatigue Life on Lower Suspension Arm Subjected to Variable Amplitude Loading*, National Conference in Mechanical Engineering Research & Postgrad Studies (2nd NCMER), Faculty of Mechanical Engineering, UMP Pekan, Kuantan, Pahang, Malaysia, p.100-116.

[11] Maksimovic, S. (2005). *Fatigue Life Analysis of Aircraft Structural Component*, Scientific-Technical Review, Volume 55, No. 1, p.15-22.

[12] Roylance, D. (2001) *Fatigue*, Department of Material Science and Engineering, Massachusetts Institute of Technology, Cambridge.

[13] Stephens, R.I., Fatemi. A., Stepehen, R.R., & Fuchs, H.O. (2000). *Cyclic Deformation and the strain-life approach*, Metal Fatigue in Engineering, 2nd Edition, John Wiley & sons, p.114

[14] Teng, T.L. & Cheng, P.H. (2003). *Fatigue crack Initiation Life Prediction for a Flat Plate with a Central Hole*, Journal of C.C.I.T, vol.32, No.1, November 2003.

[15] Topper, T.H., Wetzel, R.M., & Morrow, J. (1969). *Neuber's Rule Applied to Fatigue of Notched Specimen*, Journal of Materials, Volume 4, No.1.

[16] Vreudge, E. (2001). *Metal Fatigue: A summary of Cases and Cures*, Technical Brief Number 14, Metserve International, South Africa.

[17] Young, W.C., Budynas, R.G. & Sadegh, A.M. (2012). *Neuber's Rule*, Effective Stress Concentration Factors, Chapter 6: Stress Concentration, Roark's Formula for Stress and Strain, 8th Edition, McGraw-Hill Companies Inc., p.261

APPENDICES

No.	σ_a a[MPa]	ε_a a
1.	0	0
2.	50	$2.38\cdot10^{-4}$
3.	100	$4.761\cdot0^{-4}$
4.	150	$7.16\cdot10^{-4}$
5.	200	$9.66\cdot10^{-4}$
6.	250	$1.26\cdot10^{-3}$
7.	300	$1.71\cdot10^{-3}$
8.	300	$1.71\cdot10^{-3}$
9.	350	$2.56\cdot10^{-3}$
10.	400	$4.32\cdot10^{-3}$
11.	450	$7.96\cdot10^{-3}$
12.	500	$1.52\cdot10^{-2}$
13.	550	$2.861\cdot0^{-2}$
14.	650	$9.36\cdot10^{-2}$

Appendix 1: Cyclic stress-strain plot for SAE1045 from Maksimovic's *Fatigue Life Analysis of Aircraft Structural Component* paper

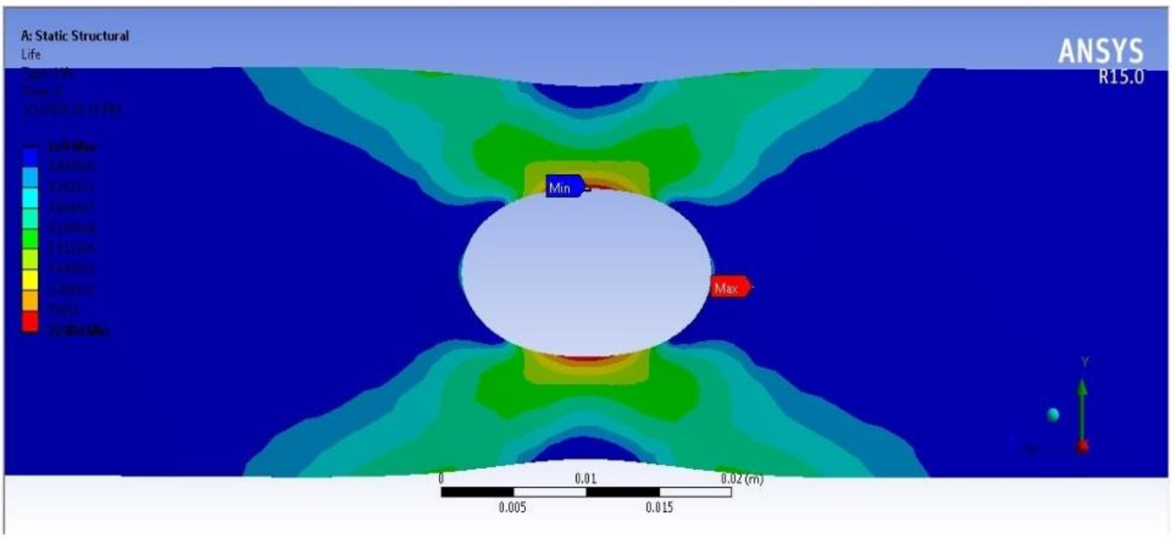

Appendix 2: Distribution of life cycle, N_{fi} within the model of plate-with-hole under cyclic loading of 25.57kN (S_{max} = 130.56MPa)

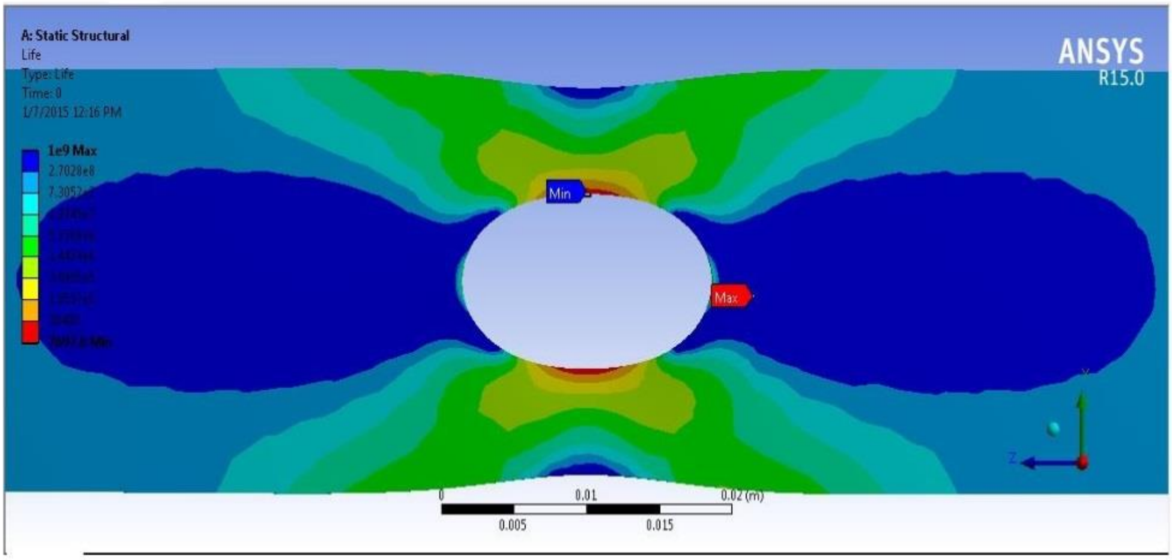

Appendix 3: Distribution of life cycle, N_{fi} within the model of plate-with-hole under cyclic loading of 31.14kN (S_{max} = 160.91MPa)

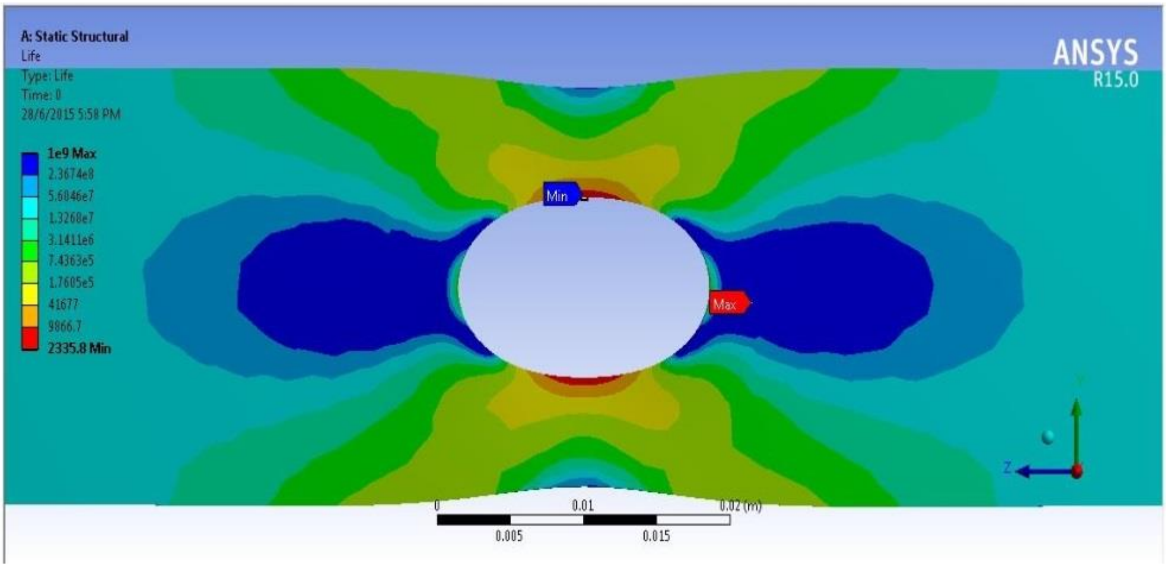

Appendix 4: Distribution of life cycle, N_{fi} within the model of plate-with-hole under cyclic loading of 40.18kN (S_{max} = 207.60MPa)

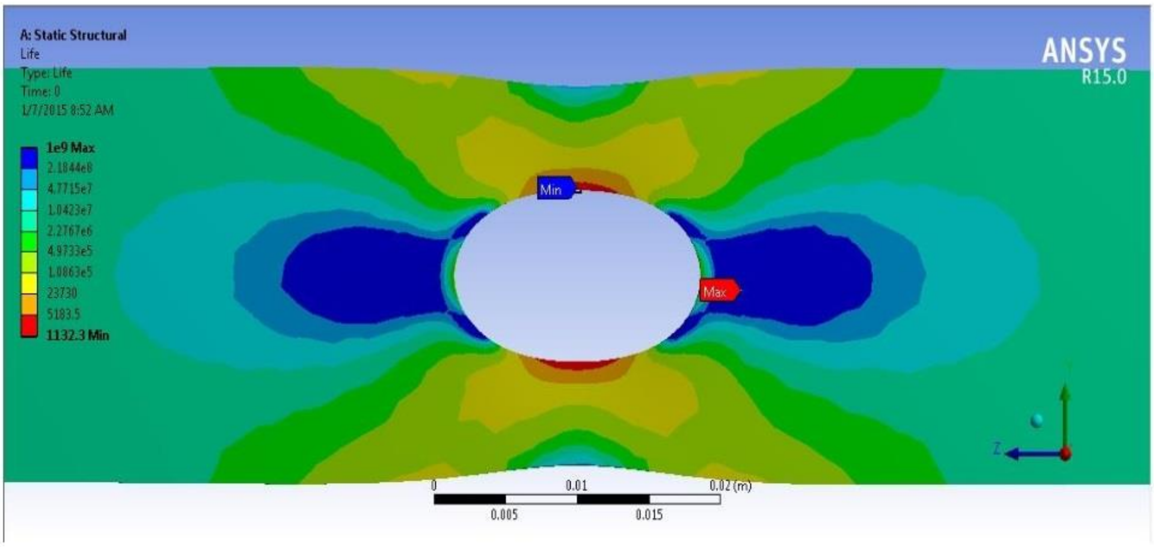

Appendix 5: Distribution of life cycle, N_{fi} within the model of plate-with-hole under cyclic loading of 40.18kN (S_{max} = 207.60MPa)

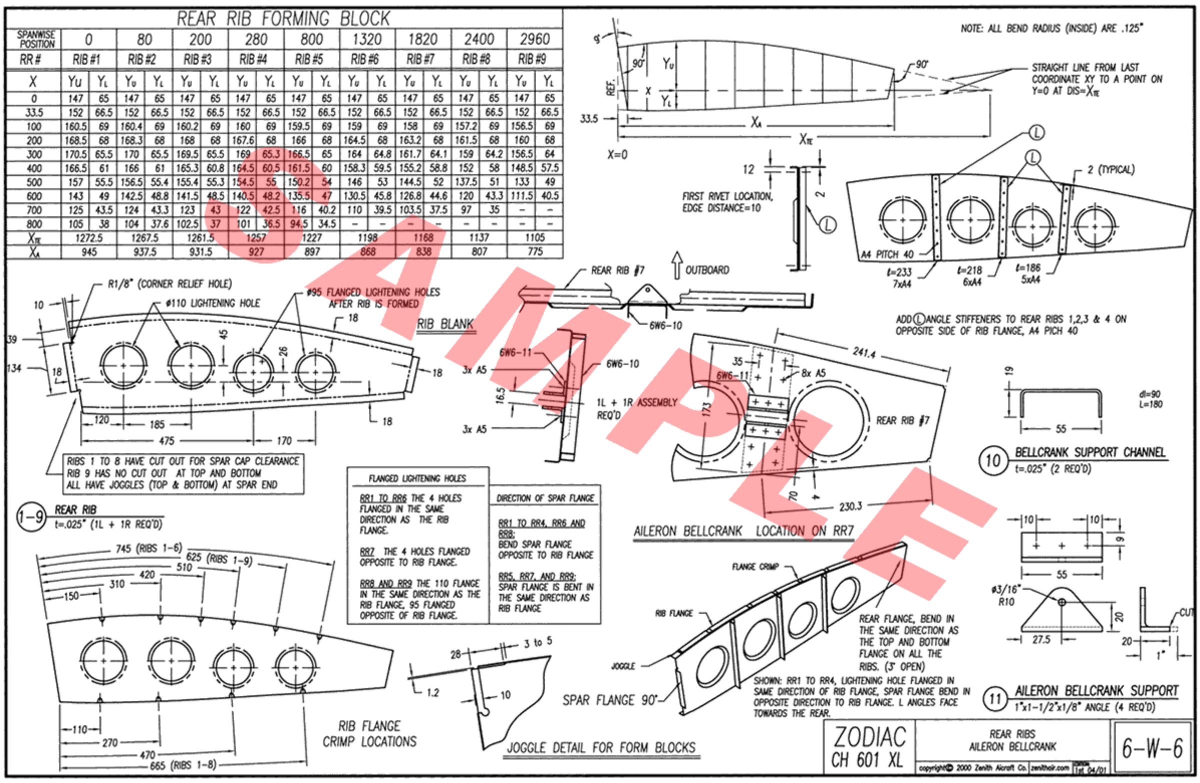

Appendix 6: Zenair CH601XL wing rib drawing

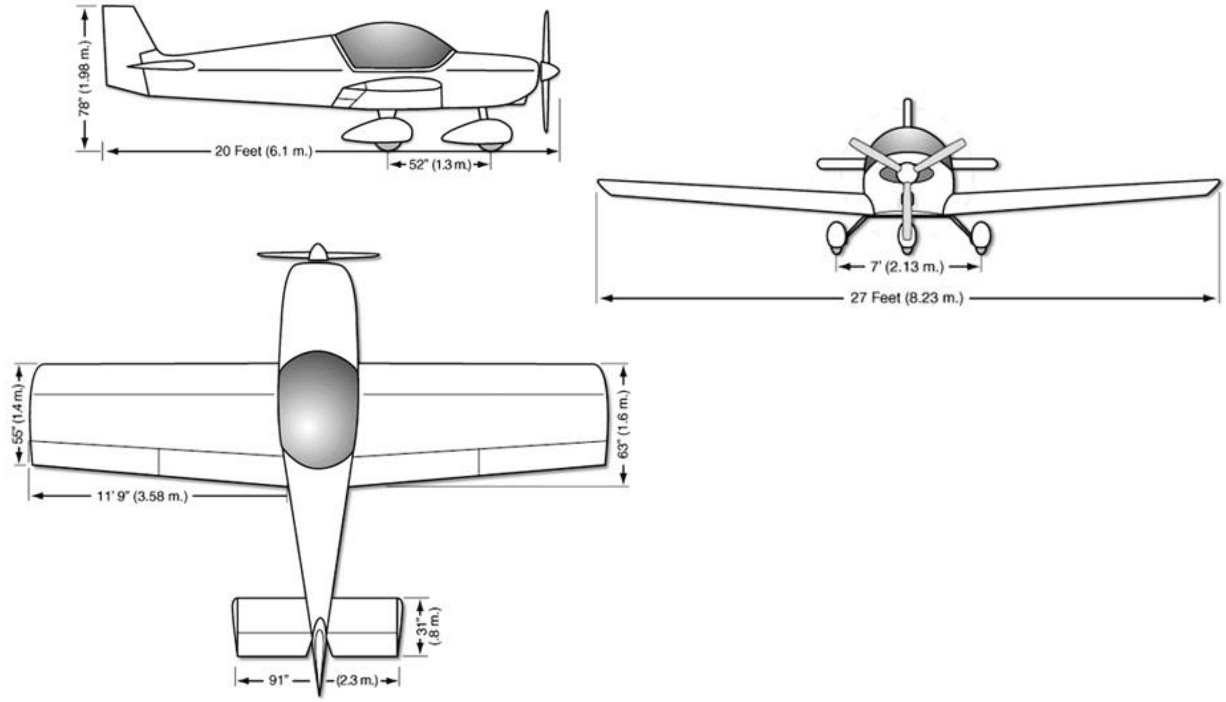

Appendix 7: Zenair CH601XL dimensions

Stall speed (Vs):	44
Normal operations speed:	44-125
Maneuvering speed (Va):	97
Caution range:	112 - 150
Never exceed speed (Vne):	150

Appendix 8: Zenair CH601XL Operational limits

	ROTAX 912 (80 HP)	
WING SPAN	27	FEET
WING AREA	130	SQ. FT.
LENGTH	19	FEET
EMPTY WEIGHT	550	LBS.
USEFUL LOAD	508	LBS.
GROSS WEIGHT	1058	LBS.
WING LOADING	8.0	P.S.F.
POWER LOADING	13.1	HP / LBS.
CABIN WIDTH	44	INCHES
FUEL CAPACITY (STANDARD)	16	US GAL.
– PLUS WING TANKS (OPTIONAL)	2 x 7.5	US GAL.

Appendix 9: Zenair CH601XL Specifications

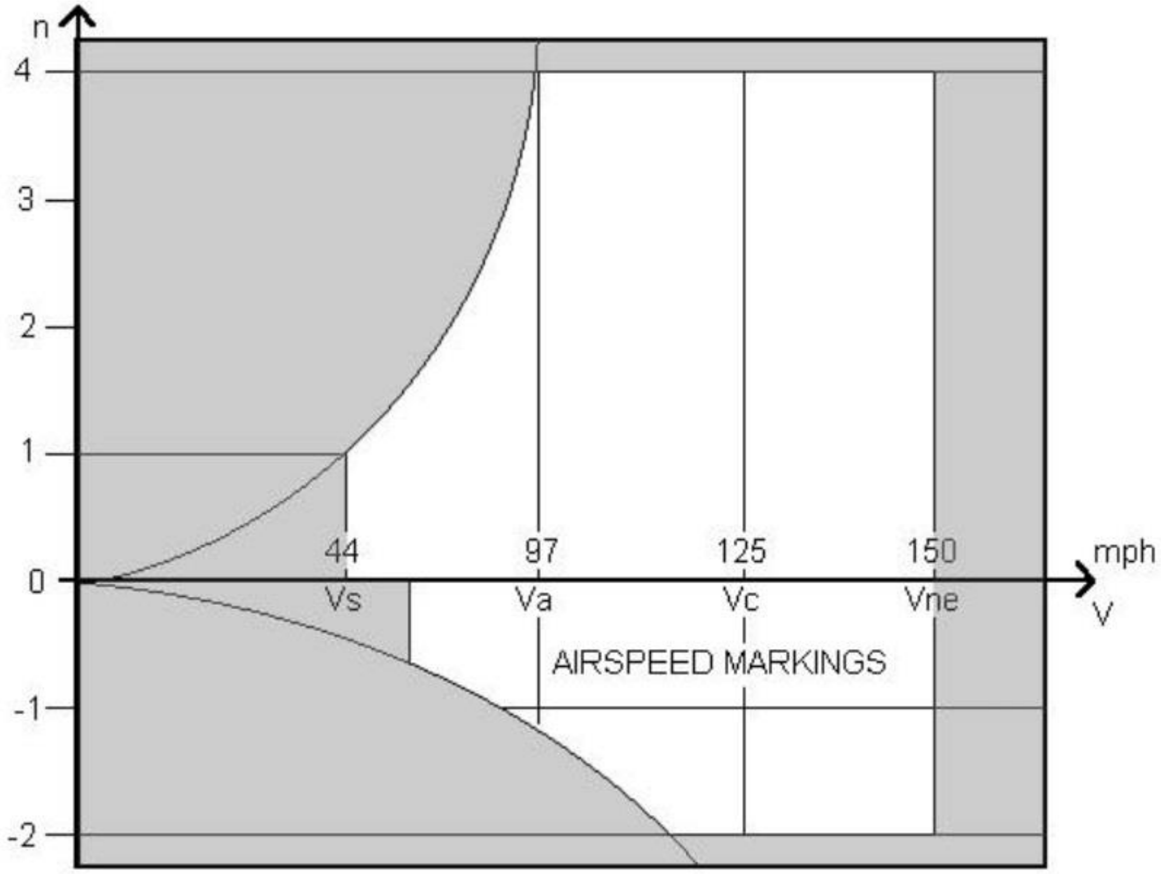

Appendix 10: Zenair CH601XL flight envelope